DEPARTMENT OF OCEAN, EARTH, AND ATMOSPHERIC SCIENCES
COLLEGE OF SCIENCES
OLD DOMINION UNIVERSITY
NORFOLK, VA 23529

DISTURBANCE DYNAMICS IN TRANSITIONAL AND TURBULENT FLOWS

By
Dr. Chester E. Grosch, Principal Investigator
Department of Ocean, Earth and Atmospheric Sciences

FINAL REPORT

For the period ending November 1, 1999

Prepared for
NASA Langley Research Center
Attn: Mr. Thomas B. Gatski
Technical Officer
Mail Stop 128
Hampton, VA 23681-2199

Under
NASA Research Grant No. NAG-1-2121
ODURF File No. 191141

October 1999

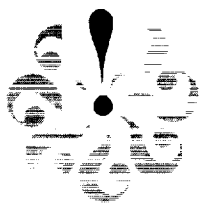

DEPARTMENT OF OCEAN, EARTH, AND ATMOSPHERIC SCIENCES
COLLEGE OF SCIENCES
OLD DOMINION UNIVERSITY
NORFOLK, VA 23529

DISTURBANCE DYNAMICS IN TRANSITIONAL AND TURBULENT FLOWS

By
Dr. Chester E. Grosch, Principal Investigator
Department of Ocean, Earth and Atmospheric Sciences

FINAL REPORT

For the period ending November 1, 1999

Prepared for
NASA Langley Research Center
Attn: Mr. Thomas B. Gatski
Technical Officer
Mail Stop 128
Hampton, VA 23681-2199

Under
NASA Research Grant No. NAG-1-2121
ODURF File No. 191141

October 1999

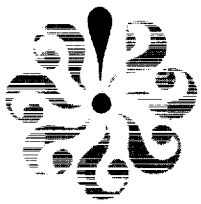

Final Report

NASA Research Grant No. NAG-1-2121
ODURF No. 191141

Disturbance Dynamics in Transitional and Turbulent Flow

By
Dr. Chester E. Grosch, Principal Investigator
Department of Ocean, Earth, and Atmospheric Sciences
Old Dominion University

Submitted by
Old Dominion University
Research Foundation
800 West 46th Street
Norfolk, Virginia 23508

Submitted to
NASA Langley Research Center
Hampton, VA 23681-2199

October 1999

Disturbance Dynamics in Transitional and Turbulent Flows

C.E. Grosch

Old Dominion University, Norfolk, Virginia 23529

ABSTRACT

In order to expand the predictive capability of single-point turbulence closure models to account for the early-stage transition regime, a methodology for the formulation and calibration of model equations for the ensemble-averaged disturbance kinetic energy and energy dissipation rate is presented. First the decay of laminar disturbances and turbulence in mean shear-free flows is studied. In laminar flows, such disturbances are linear superpositions of modes governed by the Orr-Sommerfeld equation. In turbulent flows, disturbances are described through transport equations for representative mean quantities. The link between a description based on a deterministic evolution equation and a probability based mean transport equation is established. Because an uncertainty in initial conditions exists in the laminar as well as the turbulent regime, a probability distribution must be defined even in the laminar case. Using this probability distribution, it is shown that the exponential decay of the linear modes in the laminar regime can be related to a power law decay of both the (ensemble) mean disturbance kinetic energy and the dissipation rate. The evolution of these mean disturbance quantities is then described by transport equations similar to those for the corresponding turbulent decaying flow. Second, homogeneous shear flow, where disturbances can be described by rapid distortion theory (RDT), is studied. The relationship between RDT and linear stability theory is exploited in order to obtain a closed set of modeled equations. The linear disturbance equations are solved directly so that the numerical simulation yields a database from which the closure coefficients in the ensemble-averaged disturbance equations can be determined.

1 Introduction

Demands on the range of applicability of turbulence modeling are increasing, and with these increasing demands has come the need to develop transition models within the context of the traditional Reynolds-averaged turbulence modeling. Such transition models would encompass the laminar/transitional regimes, along with the turbulent regime, describing averaged flow properties such as the mean disturbance energy and dissipation rate. In order to develop a transition/turbulence model for wall-bounded flows, which uses the strategy of employing an intermittency function that interpolates between the laminar regime with its linear disturbances and the fully turbulent regime with its stochastic fluctuations, a consistent mathematical description of the two regimes is necessary.

In all flow regimes, disturbances are defined here as deviations from the ensemble mean. The laminar regime is defined as the region of the flow in which the ensemble mean velocity (zero in the case of the homogeneous flows considered in this study) corresponds to a stationary solution of the Navier-Stokes equation, and disturbances from this mean velocity are small enough in amplitude that their nonlinear interactions can be neglected. In this regime, the evolution of the disturbances is completely predictable from their initial state. Traditionally in laminar stability theory, disturbance fields are studied through the linear Orr-Sommerfeld equation, which describes the evolution of individual infinitesimal disturbance modes. Even when a quantity, such as the disturbance energy, is studied, it is the evolution of the instantaneous quantity rather than an ensemble average that is investigated. In contrast, the turbulent regime is defined as the region where the flow is subject to stochastic fluctuations, arising from nonlinear interactions, which render the behavior of the disturbances unpredictable. In this case the disturbance field is studied through (modeled) transport equations which describe the evolution of mean turbulent correlations. The purpose of this study is to reconcile these two apparently disparate approaches through a common mathematical analysis.

While the Orr-Sommerfeld equation accounts for viscous effects on disturbances, it neglects the influence of any nonlinear interactions. The behavior of finite-amplitude disturbances can be different and is more complex since nonlinear interactions occur. However, the intent here is to analyze, within the framework of (ensemble) mean disturbance transport equations, the behavior of the linear disturbance fields which characterize the beginning of a transition process, and ultimately lead to a fully turbulent field. The approach taken here is based on the observation that even in the laminar regime every flow is subject to an inevitable uncertainty in initial conditions. Therefore, although each individual disturbance evolves deterministically, a probability distribution must be introduced for the calculation of ensemble mean properties. This approach is similar to rapid distortion theory (RDT) in that it is based on linearized disturbance equations; however, the physical interpretation is different. RDT considers flows in which turbulence is fully developed and uses linearized equations to study the behavior of the disturbances under rapid distortion. RDT is usually applied to short time evolution and the effect of viscosity is neglected. In the approach taken here, there is no limitation on the period

of time evolution as long as the disturbances remain small, and the effect of viscosity is essential. Thus linear disturbances are considered in the early stages of transition where viscous effects must be taken into account.

More recent extensions of RDT by Salhi, Cambon and Speziale (1997) have also exploited the connection with linear stability theory. They studied quadratic flows in a rotating frame to gain better insight into the dynamics so that a generalized stability criterion applicable to turbulent flows could be developed. They also considered the effect on single-point closure modeling – specifically the deficiencies in predicting elliptic flows. While the mathematical framework is similar in this study, the region of interest here is the early-stage transition regime. Nevertheless, this commonality further substantiates the basic assumption that a mathematical framework can be developed which will provide a set of transport equations capable of describing the flow (in a mean statistical sense) in the early-stage transition regime.

First the decay of laminar disturbances and turbulence in mean shear-free flows is studied. The study of homogeneous turbulence has become an essential element in the calibration of turbulence closure models. The simplest of the homogeneous flows is decaying, isotropic turbulence, which traditionally has been used to determine the destruction coefficient in the modeled dissipation rate equation used in two-equation and higher-order closure models.

In the second part the case of mean homogeneous shear is studied. Homogeneous shear flow is commonly used as a calibration flow for turbulence models because both turbulent transport and viscous terms can be removed from the transport equations for the turbulent correlations. An extensive amount of experimental (Tavoularis and Corrsin, 1981, Tavoularis and Karnik,1989) and numerical simulation data (Rogers and Moin, 1987) at low and moderate shear also exists which further aids in its role as a turbulent calibration flow.

The purpose of this entire study is to use the solution of the disturbance evolution equations for mean shear-free and mean homogeneous shear flows as a database in the calibration of the evolution equations for the ensemble-averaged disturbance correlations. As a beginning, the focus is on a simple disturbance kinetic energy and disturbance dissipation rate (two-equation) description. In such a two-equation description of homogeneous shear, the terms in the kinetic energy equation are exact and require no modeling; whereas, in the dissipation rate equation both the production-of-dissipation and destruction-of-dissipation terms require modeling. The two closure coefficients associated with these terms are determined from the analysis presented here. Utilization of the disturbance evolution results as a reliable database is supported by the DNS results of Lee, Kim, and Moin (1990) who studied homogeneous shear flow at a high-shear rate. They showed that RDT results compared very well with the simulation results over the time period examined. The results herein also show good agreement with the DNS results (Lee, *et al*, 1990), and are found to apply at much later times due to the energetic decay of the disturbance field in the parameter range studied. Thus, this database will be used to provide insight into the asymptotic behavior of important dynamic variables, as well as to provide the necessary information for the closure model calibration. The resulting closed disturbance dissipation rate equation can then be used in the formulation of a transition-sensitized turbulence model.

2 Boundary-Free Disturbance Fields

Consider first the case of disturbances in a laminar, zero mean-shear flow with no boundaries. Solid boundaries do indeed play a key role in the dynamics of any laminar disturbances and the transition process itself; however, in order to establish the mathematical framework, this first example will be unbounded, as is the decaying homogeneous turbulent flow. For this initial-value problem, an arbitrary solution of the Orr-Sommerfeld equation (here, the linearized Navier-Stokes equations) is given by

$$u_i(\mathbf{x},t) = \int d^3\mathbf{k}\, u_i^0(\mathbf{k}) e^{(i\mathbf{k}\cdot\mathbf{x} - \nu k^2 t)}, \tag{1}$$

where $\mathbf{k} = (k_1, k_2, k_3)$ is the wavenumber vector in the coordinate directions $\mathbf{x} = (x, y, z)$, respectively, and ν is the kinematic viscosity. Because the initial conditions are uncertain, an ensemble of such disturbances is considered for which a probability distribution can be ascribed to the initial mode amplitudes, $u_i^0(\mathbf{k})$. The mean of this distribution is zero and the covariance is $\left\langle u_i^0(\mathbf{k}) u_j^0(\mathbf{k}')\right\rangle$. The corresponding two-point correlation function of the disturbance field is then

$$\langle u_i(\mathbf{x},t) u_j(\mathbf{x}',t)\rangle = \int d^3\mathbf{k} d^3\mathbf{k}' \left\langle u_i^0(\mathbf{k}) u_j^0(\mathbf{k}')\right\rangle e^{i(\mathbf{k}\cdot\mathbf{x}+\mathbf{k}'\cdot\mathbf{x}')} e^{-\nu(k^2+k'^2)t} \tag{2}$$

where $\mathbf{x}' = \mathbf{x} + \mathbf{r}$, and the homogeneity of $\langle u_i(\mathbf{x},t) u_j(\mathbf{x}',t)\rangle$ implies that

$$\left\langle u_i^0(\mathbf{k}) u_j^0(\mathbf{k}')\right\rangle = \delta^3(\mathbf{k}+\mathbf{k}') f_{ij}(\mathbf{k}). \tag{3}$$

The two-point correlation function is then given in the form

$$R_{ij}(\mathbf{r},t) = \int d^3\mathbf{k} f_{ij}(\mathbf{k}) e^{i\mathbf{k}\cdot\mathbf{r} - 2\nu k^2 t}, \tag{4}$$

with the corresponding energy spectrum tensor

$$E_{ij}(\mathbf{k},t) = f_{ij}(\mathbf{k}) e^{-2\nu k^2 t}, \tag{5}$$

which is assumed to be analytic at the origin (Hinze, 1975). This yields a wavenumber distribution for f_{ij} which satisfies both isotropy and incompressibility,

$$f_{ij}(\mathbf{k}) = \left(k^2\delta_{ij} - k_i k_j\right) f(k^2), \tag{6}$$

where $f(k^2)$ is a nonsingular, scalar function which can be related to the mean disturbance kinetic energy through

$$K(t) = \frac{1}{2}\int d^3\mathbf{k}\; E_{ii}(\mathbf{k},t) = \int d^3\mathbf{k}\; f(k^2) k^2 e^{-2\nu k^2 t}. \tag{7}$$

In general, $f(k^2)$ must go to zero sufficiently rapidly at infinity so that the integral in (7) is finite at $t = 0$. A natural choice for $f(k^2)$ is the normal distribution $\exp(-ak^2)$. With this choice of $f(k^2)$, Eq. (7) then gives the mean disturbance kinetic energy

$$K(t) = K_0 \left(1 + \frac{2\nu}{a} t\right)^{-5/2}, \tag{8}$$

where K_0 is the initial value of K. Recall that for decaying homogeneous turbulence, the power law behavior for the final period of decay (Hinze, 1975; Batchelor and Proudman, 1956), is $K(t) \propto t^{-5/2}$. Thus, the decaying linear disturbances have the same temporal character as turbulence in the final period of decay.

The covariance of the initial mode amplitudes given in (3) can then be written explicitly as

$$\left\langle u_i^0(\mathbf{k}) u_j^0(\mathbf{k}') \right\rangle = \delta^3(\mathbf{k}+\mathbf{k}') \left(\delta_{ij} - \frac{k_i k_j}{k^2} \right) K_0 \mathcal{P}(\mathbf{k}), \tag{9}$$

where

$$\mathcal{P}(\mathbf{k}) = \frac{2}{3} \left(\frac{a^5}{\pi^3} \right)^{1/2} k^2 e^{-ak^2} \tag{10}$$

is a probability distribution for the disturbance second-moments, normalized so that $\int d^3\mathbf{k}\mathcal{P}(\mathbf{k}) = 1$, and a is related to the variance of the distribution. With this distribution $\mathcal{P}(\mathbf{k})$, other second-moments can be calculated. For example, the ensemble mean energy dissipation rate

$$\varepsilon = \nu \left\langle \frac{\partial u_i}{\partial x_j} \left(\frac{\partial u_i}{\partial x_j} + \frac{\partial u_j}{\partial x_i} \right) \right\rangle \tag{11}$$

can be written as

$$\begin{aligned} \varepsilon &= -\nu \int d^3\mathbf{k} d^3\mathbf{k}' e^{i(\mathbf{k}+\mathbf{k}')\cdot\mathbf{x}} e^{-\nu(k^2+k'^2)t} \left[\left\langle u_i^0(\mathbf{k}) u_i^0(\mathbf{k}') \right\rangle k_j k_j' + \left\langle u_i^0(\mathbf{k}) u_j^0(\mathbf{k}') \right\rangle k_j k_i' \right] \\ &= 2\nu K_0 \int d^3\mathbf{k}\, k^2 e^{-2\nu k^2 t} \mathcal{P}(\mathbf{k}) = \frac{5\nu}{a} K_0 \left(1 + \frac{2\nu t}{a} \right)^{-7/2} \end{aligned} \tag{12}$$

which, for this decaying flow, is simply given by the time derivative of the disturbance kinetic energy in (8), that is, $\dot{K} = -\varepsilon$.

It is well known that for any power law decay of the mean disturbance kinetic energy, with power $-p$, the mean disturbance dissipation rate equation

$$\dot{\varepsilon} = -C_{\varepsilon 2} \frac{\varepsilon^2}{K}. \tag{13}$$

is satisfied exactly, and the coefficient $C_{\varepsilon 2}$ is given by

$$C_{\varepsilon 2} = 1 + \frac{1}{p}. \tag{14}$$

For this case of mean, laminar shear-free flow with no boundaries, the coefficient $C_{\varepsilon 2}$ is then 1.40. In the turbulent case, values in the range of $1.80 - 2.00$ have been deduced from experiments (Batchelor and Townsend, 1948; Comte-Bellot and Corrsin, 1966; Comte-Bellot and Corrsin, 1971), although the values more commonly used are delimited by $1.83 - 1.92$.

In the turbulence case, there has been a considerable amount of research associated with the proper choice of decay rate (Frisch, 1995; Lesieur, 1995). The values obtained have ranged from a power law decay with exponent $-6/5$ (corresponding to a k^2 low wavenumber behavior of the

energy spectrum $E(k) \propto k^2 E_{ii}(\mathbf{k})$) to a power law decay with exponent $-10/7$ (Kolmogorov decay law corresponding to a k^4 low wavenumber behavior). In the laminar disturbance case, the temporal and the wavenumber dependence of the energy spectrum tensor are both given explicitly from the disturbance mode solutions of the Orr-Sommerfeld equation together with a probability distribution. The probability distribution enforces analyticity at $\mathbf{k} = \mathbf{0}$ and goes to zero sufficiently rapidly at infinity so that the integrals exist. A simple integration over wavenumbers then yields the decay law of the disturbance kinetic energy with exponent $-5/2$, in agreement with the final period of decay for the fully turbulent case. This agreement is not surprising, because in the final period of decay, viscous effects are dominant, with the small scale (high wavenumber) turbulence already decayed away.

3 Wall-Bounded Disturbance Fields

While it is encouraging to have identified a relationship between the decaying linear disturbances and decaying turbulence in the boundary-free flow, a wall-bounded flow is more relevant for an analysis of linear disturbances which evolve through a transition stage and then into full turbulence. Shear-free decaying turbulent flows with boundaries have been the focus of experimental, (Uzkan and Reynolds, 1967; Thomas and Hancock, 1977) theoretical, (Hunt and Graham, 1978) and numerical simulation (Perot and Moin, 1995) studies. The motivation for these studies was to assess the inhibiting effect on the turbulent fluctuations due to the presence of the wall in the absence of any mean shear arising from the relative motion between the mean flow and the wall. Here, the corresponding case of disturbances in a laminar, zero mean-shear flow with a boundary will be studied. For laminar disturbances, the wall has the effect of fixing the phase of the Orr-Sommerfeld modes in the wall-normal direction.

The wall-normal direction is the y direction, and the wall boundary is located in the (x, z) plane at $y = 0$. In this flow, the modes are given by

$$\hat{u}_i(y, \mathbf{k}) e^{i(\mathbf{k}\cdot\mathbf{x} - \omega t)}, \tag{15}$$

where now $\mathbf{k} = (k_1, 0, k_3)$ is the wavenumber vector in the coordinate directions (x, y, z), respectively, and ω is the complex frequency of the disturbances. An analysis (Grosch and Salwen, 1978) of the Orr-Sommerfeld equation shows that bounded solutions only exist when ω is pure imaginary ($\omega = i\omega_i$, $i = \sqrt{-1}$) and

$$\omega_i = -(1 + \lambda)\nu k^2 < -\nu k^2, \tag{16}$$

where the parameter $\lambda(> 0)$ has been introduced. For three-dimensional disturbances, Squire's transformation is used, and the Orr-Sommerfeld equation determines the velocity disturbances $\hat{u}_2$ and $k_1\hat{u}_1 + k_3\hat{u}_3$. The individual disturbance components, $\hat{u}_1$ and $\hat{u}_3$, can then be determined in one of two ways. First, the pressure field can be determined from the linearized $\hat{u}_2$ momentum equation and then substituted into both the $\hat{u}_1$ and $\hat{u}_3$ linearized momentum equations. Second,

the kinematic equation for the y component of vorticity $i(k_3\hat{u}_1 - k_1\hat{u}_3)$ can be coupled with the relation between $\hat{u}_2$ and $(k_1\hat{u}_1 + k_3\hat{u}_3)$ from the Orr-Sommerfeld equation to determine $\hat{u}_1$ and $\hat{u}_3$ individually. Because the solution for $(k_1\hat{u}_1 + k_3\hat{u}_3)$ and $\hat{u}_2$ obtained from the Orr-Sommerfeld equation is an irrotational wave of arbitrary amplitude, and the solution of the vorticity equation has an independent amplitude, it is necessary to introduce a new parameter, μ, for the ratio of these two amplitudes. The component disturbance modes are then given by

$$\hat{u}_1(y,\mathbf{k}) = i\left[\frac{k_1}{k}\cos(\sqrt{\lambda}ky) + \left(\sqrt{\lambda}\frac{k_1}{k} - \mu\frac{k_3}{k}\right)\sin(\sqrt{\lambda}ky) - \frac{k_1}{k}e^{-ky}\right], \tag{17}$$

$$\hat{u}_2(y,\mathbf{k}) = \left[-\cos(\sqrt{\lambda}ky) + \frac{1}{\sqrt{\lambda}}\sin(\sqrt{\lambda}ky) + e^{-ky}\right], \tag{18}$$

$$\hat{u}_3(y,\mathbf{k}) = i\left[\frac{k_3}{k}\cos(\sqrt{\lambda}ky) + \left(\sqrt{\lambda}\frac{k_3}{k} + \mu\frac{k_1}{k}\right)\sin(\sqrt{\lambda}ky) - \frac{k_3}{k}e^{-ky}\right], \tag{19}$$

where $k = \sqrt{k_1^2 + k_3^2}$ because $k_2 = 0$. At the wall where the no-slip condition is applied, $\hat{u}_i = 0$, and far from the wall in the freestream, where $e^{-ky} \to 0$, the modes $\hat{u}_i$ are periodic functions of y. It should be recognized that these expressions for the velocity components, because of the no-slip wall boundary conditions, have fixed the phase of the disturbances in the y-direction. In the absence of the wall boundary condition, the exponential terms would not appear and the phase would remain arbitrary in this direction.

The component disturbance modes (17) – (19) form a complete set (Salwen and Grosch, 1981) of non-normalizable eigenfunctions. A disturbance in the laminar regime is a linear combination of these eigenfunctions

$$u_i(\mathbf{x},t) = \int d\lambda\, d\mu\, d^2\mathbf{k}\, \Phi(\lambda,\mu,k_1,k_3)\hat{u}_i(y,\mathbf{k})e^{[i\mathbf{k}\cdot\mathbf{x} - (1+\lambda)\nu k^2 t]}, \tag{20}$$

which is normalizable in accordance with the finiteness of the disturbance kinetic energy. In Eq. (20), the initial mode amplitude $\Phi(\lambda,\mu,k_1,k_3)$ is again an element of an ensemble with mean zero and covariance $\langle\Phi^*(\lambda,\mu,k_1,k_3)\Phi(\lambda',\mu',k',k')\rangle$. Since the modes $\hat{u}_i$ are complex, the two-point correlation function is the real part of

$$\langle u_i^*(\mathbf{x},t)u_j(\mathbf{x}',t)\rangle = \int d\lambda\, d\mu\, d\lambda'\, d\mu' d^2\mathbf{k}\, d^2\mathbf{k}'\, \langle\Phi^*(\lambda,\mu,k_1,k_3)\Phi(\lambda',\mu',k',k')\rangle \cdot\hat{u}_i^*(y,\mathbf{k})\hat{u}_j(y',\mathbf{k}')e^{i(\mathbf{k}'\cdot\mathbf{x}' - \mathbf{k}\cdot\mathbf{x})}e^{-\nu[(1+\lambda)k^2 + (1+\lambda')k'^2]t} \tag{21}$$

where $*$ quantities denote complex conjugates. Homogeneity in the x_1 and x_3 directions then implies that $\langle\Phi^*(\lambda,\mu,k_1,k_3)\Phi(\lambda',\mu',k',k')\rangle$ contains $\delta(k_1 - k')\delta(k_3 - k')\mathcal{P}(k_1,k_3)$ where, due to invariance under rotations about the y-axis, $\mathcal{P}(k_1,k_3)$ is a function of k^2. It is still necessary to fix the dependence of the covariance $\langle\Phi(\lambda,\mu,k_1,k_3)\Phi^*(\lambda',\mu',k',k')\rangle$ on $(\lambda,\mu,\lambda',\mu')$. This is done by imposing an appropriate isotropy condition in the freestream, where the decaying exponentials can be set equal to zero in the component disturbance mode equations (17) – (19). In the boundary-free case, the disturbance field is isotropic, and the ensemble mean square of the three velocity components and of the three vorticity components are equal at each point throughout

the domain. In the bounded case, the wall fixes the phases of the laminar disturbances in the y direction even for large values of y, and it is not possible to impose pointwise isotropy as a condition on an ensemble of such disturbances. However, for large values of y (freestream), a weaker form of isotropy can be imposed on the disturbance field by averaging over the y direction. Specifically, this requires that in the freestream the ensemble mean square of the three velocity components and of the three vorticity components, integrated over y, be equal. The simplifying assumption must also be made that $\langle \Phi(\lambda,\mu,k_1,k_3)\Phi^*(\lambda',\mu',\mathbf{k}')\rangle$ is diagonal in λ and μ so that

$$\langle \Phi(\lambda,\mu,k_1,k_3)\Phi^*(\lambda',\mu',\mathbf{k}')\rangle = \delta(\lambda'-\lambda)\delta(\mu'-\mu)\delta^2(\mathbf{k}-\mathbf{k}')\mathcal{P}(k_1,k_3)\; p(\lambda,\mu) \tag{22}$$

where the function $p(\lambda,\mu)$ remains to be determined from the isotropy conditions. Taking y_1 sufficiently large that $e^{-ky} \approx 0$ for $y \geq y_1$, one obtains from (17) - (19)

$$\lim_{L\to\infty}\frac{1}{L}\int_{y_1}^{y_1+L} dy \left\langle |u_1(\mathbf{x},t)|^2 \right\rangle = \int dk_1 dk_3 d\lambda d\mu \mathcal{P}(k_1,k_3)p(\lambda,\mu) \cdot\frac{1}{2}\left[(1+\lambda)\frac{k_1^2}{k^2}+\mu^2\frac{k_3^2}{k^2}\right] e^{-2(1+\lambda)\nu k^2 t} \tag{23}$$

$$\lim_{L\to\infty}\frac{1}{L}\int_{y_1}^{y_1+L} dy \left\langle |u_2(\mathbf{x},t)|^2 \right\rangle = \int dk_1 dk_3 d\lambda d\mu \mathcal{P}(k_1,k_3)p(\lambda,\mu) \cdot\frac{1}{2}\left(1+\frac{1}{\lambda}\right) e^{-2(1+\lambda)\nu k^2 t} \tag{24}$$

$$\lim_{L\to\infty}\frac{1}{L}\int_{y_1}^{y_1+L} dy \left\langle |u_3(\mathbf{x},t)|^2 \right\rangle = \int dk_1 dk_3 d\lambda d\mu \mathcal{P}(k_1,k_3)p(\lambda,\mu) \cdot\frac{1}{2}\left[(1+\lambda)\frac{k_3^2}{k^2}+\mu^2\frac{k_1^2}{k^2}\right] e^{-2(1+\lambda)\nu k^2 t} \tag{25}$$

where the integration over y has eliminated the cross terms $\cos(\sqrt{\lambda}ky)\sin(\sqrt{\lambda}ky)$, while $\sin^2(\sqrt{\lambda}ky)$ and $\cos^2(\sqrt{\lambda}ky)$ have each yielded an average of $1/2$. The terms containing k_1k_3 have also vanished since $\mathcal{P}(k_1,k_3)$ is even in k_1 and in k_3. According to the assumed isotropy, the function $p(\lambda,\mu)$ must have the property that the right hand sides of Equations (23)-(25) must be equal. The condition that averaged over y, $\langle |u_1|^2\rangle = \langle |u_3|^2\rangle$ is satisfied automatically, while the condition $\langle |u_1|^2\rangle = \langle |u_2|^2\rangle$ yields the relation

$$\frac{1}{2}\left(1+\lambda+\mu^2\right) = 1+\frac{1}{\lambda}\,, \tag{26}$$

where use has been made of the identity

$$\int d^2\mathbf{k}k_1^2F(k^2) = \int d^2\mathbf{k}k_3^2F(k^2) = \frac{1}{2}\int d^2\mathbf{k}k^2F(k^2) \tag{27}$$

when F is any function of k^2 for which the integral exists. Calculating the vorticity $\omega_j(\mathbf{x},t)$ from the modes $\hat{u}_i(y,\mathbf{k})e^{(i\mathbf{k}\cdot\mathbf{x}\;-\;(1+\lambda)\nu k^2 t)}$, with $e^{-ky}\equiv 0$, one obtains expressions analogous to (23)-(25), for the ensemble mean square vorticity components averaged over y. Isotropy again requires

that these three mean square vorticity components are equal. The condition that, averaged over y, $\langle|\omega_1|^2\rangle = \langle|\omega_3|^2\rangle$ is satisfied for any function $p(\lambda,\mu)$, and the demand that $\langle|\omega_1|^2\rangle = \langle|\omega_2|^2\rangle$ yields the relation

$$\frac{1}{2}\left[(1+\lambda)^2 + \lambda\mu^2 + \lambda + 2 + \frac{1}{\lambda}\right] = \mu^2 \tag{28}$$

Solving (26) and (28) for positive λ and μ then gives

$$\lambda = \frac{1}{2} \quad \text{and} \quad \mu = \frac{3}{\sqrt{2}}, \tag{29}$$

which is enforced by taking

$$p(\lambda,\mu) = \delta\left(\lambda - \frac{1}{2}\right)\delta\left(\mu - \frac{3}{\sqrt{2}}\right) \tag{30}$$

The remaining function $\mathcal{P}(k_1,k_3)$ in the covariance (22) will be determined from a consideration of the two-point correlation function and the energy spectrum tensor.

Since the disturbance field is partially homogeneous, (Lumley, 1970) that is, homogeneous in the x and z directions and inhomogeneous in the y direction, the two-point correlation function is

$$R_{ij}(y,y',\mathbf{r},t) = A\int d^2\mathbf{k}\mathcal{P}(k_1,k_3)e^{i\mathbf{k}\cdot\mathbf{r}\,-\,3\nu k^2 t}\,\hat{u}_i^*(y,\mathbf{k})\hat{u}_j(y',\mathbf{k}) \tag{31}$$

where $\mathbf{r} = (x'-x, 0, z'-z)$, A is a constant proportional to the initial disturbance kinetic energy, and $\mathcal{P}(k_1,k_3)$ again plays the role of a probability distribution for the disturbance second-moments. In order to obtain explicit expressions for the components of $R_{ij}(y,y',\mathbf{r},t)$, the values for the parameters λ and μ in (29) must be substituted into the component disturbance mode equations (17)–(19). In the boundary-free case, an exponential time decay with coefficient $-2\nu k^2$ is shown in (4); whereas, in this wall-bounded case, the coefficient $-3\nu k^2$ is found. This is because of the value of λ, which is zero in the boundary-free case and 1/2 in this wall-bounded case.

An energy spectrum tensor can also be defined at each fixed y as a Fourier transform in x and z:

$$E_{ij}(y,k_1,k_3,t) = A\mathcal{P}(k_1,k_3)\hat{u}_i^*(y,\mathbf{k})\hat{u}_j(y,\mathbf{k})e^{-3\nu k^2 t}. \tag{32}$$

Once again, it is necessary that the energy spectrum be analytic at $\mathbf{k} = \mathbf{0}$. From (17)–(19), this analyticity requires that the distribution $\mathcal{P}(k_1,k_3)$ have a leading-order behavior of k^2. In addition, the finiteness of the initial disturbance energy implies that the spectrum should go to zero sufficiently rapidly for large k, specifically at $t = 0$. These requirements lead to the normalized distribution

$$\mathcal{P}(k_1,k_3) = \frac{a}{\pi}k^2 e^{-ak^2}, \tag{33}$$

where a is related to the variance of the probability distribution. Substituting the probability distribution (33), and the mode disturbance equations, (17)–(19), into the expression for

the energy spectrum tensor (32), and integrating, it is found that in the freestream the mean disturbance energy, averaged over one y wavelength, $2\pi/\sqrt{\lambda}k = 2\sqrt{2}\pi/k$, is

$$\begin{aligned} K(t) &= \frac{1}{2}\int d^2\mathbf{k}\,\frac{k}{2\sqrt{2}\pi}\int dy E_{ii}(y,k_1,k_3,t) \\ &= K_0\left(1+\frac{3\nu}{a}t\right)^{-2}, \end{aligned} \tag{34}$$

where K_0 is the initial mean disturbance energy, averaged over y. This then identifies A, introduced in the two-point correlation equation (31), as $A = 4aK_0/9$.

In the presence of a boundary, the mean disturbance energy decays according to a power law with exponent -2, in contrast to the exponent $-5/2$ obtained for the boundary-free case. The difference between the two cases arises from the fact that for bounded flow only two independent wavenumbers are integrated in (34), while the integral in (7), for boundary-free flow, contains three independent wavenumbers.

From Eq. (14) with $p = 2$, it is seen that for laminar, linear decaying disturbances in the presence of a wall, the coefficient in the mean disturbance dissipation rate equation is $C_{\varepsilon 2} = 1.5$. In the turbulent case, the experiment of Thomas and Hancock, (1977) with a turbulent Reynolds number Re_T $(= K^2/\nu\varepsilon)$ of 2000, yielded a decay law near the wall of approximately 1, which in turn gave a value for $C_{\varepsilon 2}$ of 2. The recent direct numerical simulation of Perot and Moin, (1995) with $Re_T = 137$, also displayed a decay law near the wall of approximately 1.

It may appear surprising that the wall affects the decay rate of linear disturbances infinitely far from the wall. The derivation of this result is based on the assumption that the initial disturbance field is an ensemble consisting of linear superpositions of modes which each satisfy the wall boundary condition $\hat{u}_i(0) = 0$. This boundary condition fixes the phases of the disturbances in the direction normal to the wall up to infinity, while the phases in the directions parallel to the wall are random. The situation is different for decaying isotropic turbulence, where in the initial stages of decay nonlinear interactions among the modes randomize the phases in the y-direction outside of a viscous sublayer next to the wall. Even when the turbulence has decayed to a stage where the nonlinear terms can be neglected, the phases will remain random far from the wall. For this reason, turbulence in the final stage of decay is unaffected by a wall outside of the viscous sublayer.

It is finally necessary to consider the condition for the validity of the linear approximation for decaying disturbances. Since there is no mean flow $\mathbf{U}$, one cannot impose the obvious condition $\frac{|\mathbf{u}|}{|\mathbf{U}|} \ll 1$. In the absence of mean flow, the disturbance velocity obeys the Navier-Stokes equation

$$\frac{\partial u_i}{\partial t} + u_j\frac{\partial u_i}{\partial x_j} = -\frac{\partial p}{\partial x_i} + \nu\frac{\partial^2 u_i}{\partial x_j \partial x_j}. \tag{35}$$

The nonlinear terms can be neglected when the inertial forces are much smaller than the viscous forces, that is

$$\left|u_j\frac{\partial u_i}{\partial x_j}\right| \ll \left|\nu\frac{\partial^2 u_i}{\partial x_j \partial x_j}\right|. \tag{36}$$

The scale for the amplitude of the disturbance velocity is set by the initial disturbance kinetic energy, $u_i \sim K_0^{\frac{1}{2}}$. The length scale L is determined from the probability distribution for disturbance second moments, the standard deviation fixing a wave vector scale L^{-1}. For a probability distribution of the form $k^2 e^{-ak^2}$, $L \sim a^{\frac{1}{2}}$, and the condition (36) gives a Reynolds number criterion

$$\frac{\sqrt{aK_0}}{\nu} \ll 1. \tag{37}$$

Although the parameter $a(= L^2)$ appearing in the probability distributions (10) and (33) does not affect the value of the destruction of dissipation coefficient $C_{\varepsilon 2}$, it does appear in the crucial inequality (37) which determines the validity of the linear approximation. This inequality can be expressed in terms of the disturbance Reynolds number

$$Re_d = \frac{K_0^2}{\nu \varepsilon_0} \tag{38}$$

where the initial disturbance dissipation rate ε_0 is proportional, in both the boundary-free and wall-bounded case, to $\nu K_0/a$. Thus, $Re_d \sim aK_0/\nu^2$, and the condition for the validity of the linear approximation for decaying disturbances can be expressed in the form $Re_d \ll 1$. This inequality gives a quantitative definition of linear disturbances in the laminar regime.

4 Disturbance Fields in Homogenous Shear Flow

The theoretical development here parallels that of Townsend (1970), who described the structure of turbulence in a free shear flow as a product of the finite distortion of parcels of turbulent fluid. This same RDT framework was used by Hunt and Carruthers (1990) (neglecting viscosity) to gain further insight into the structure of turbulence in shear flows and to describe some inhomogeneous flows. In this study, the relationship of RDT with linear stability theory (Speziale, Abib and Blaisdell, 1996; Salhi, Cambon and Speziale, 1997) is expanded to include an analysis of the transport equations for the ensemble-averaged disturbance kinetic energy and the disturbance energy dissipation rate. As in the turbulence case, such model equations require closure through the specification of closure constants. In the two-equation $K - \varepsilon$ formulation, only the disturbance dissipation rate equation contains modeled terms which have unknown closure constants. The homogeneous shear flow is used as a calibration flow for the production-of-dissipation and destruction-of-dissipation terms.

In terms of dimensional coordinates $(\tilde{x}_1, \tilde{x}_2, \tilde{x}_3)$ in a fixed frame, the mean velocity is given by $\tilde{U}_1 = S\tilde{x}_2$, $\tilde{U}_2 = \tilde{U}_3 = 0$, where the mean shear $S =$ constant, and the disturbance velocity and pressure are denoted by $\hat{u}_j$ and $\hat{p}$, respectively. For the problem of homogeneous shear, it is convenient to work (Rogallo, 1984) in a moving frame $(\hat{x}_1, \hat{x}_2, \hat{x}_3)$, in which the local mean velocity is zero and the coordinates are given by

$$\hat{x}_1 \;=\; \tilde{x}_1 - (\, S\hat{t}\,)\tilde{x}_2$$

$$\begin{aligned} \hat{x}_2 &= \tilde{x}_2 \\ \hat{x}_3 &= \tilde{x}_3 \ , \end{aligned} \tag{39}$$

where $\hat{t}$ is time. The mean shear S and the viscosity ν determine the time scale $T = S^{-1}$, length scale $L = \sqrt{\nu S^{-1}}$, velocity scale $U = \sqrt{\nu S}$, and pressure scale $P = U^2 = \nu S$ for the flow. This leads to the introduction of dimensionless variables $x_j = \tilde{x}_j/L$ (fixed frame), $x'_j = \hat{x}_j/L$ (moving frame), $t = \hat{t}/T$, $u_j = \hat{u}_j/U$, and $p = \hat{p}/P$.

In the moving frame, the disturbances obey the incompressibility condition

$$\frac{\partial u_1}{\partial x'_1} - t\frac{\partial u_2}{\partial x'_1} + \frac{\partial u_2}{\partial x'_2} + \frac{\partial u_3}{\partial x'_3} = 0, \tag{40}$$

and the linearized Navier-Stokes equations given by

$$\frac{\partial u_1}{\partial t} + u_2 + \frac{\partial p}{\partial x'_1} = \left(1+t^2\right)\frac{\partial^2 u_1}{\partial x'^2_1} - 2t\frac{\partial^2 u_1}{\partial x'_1 \partial x'_2} + \frac{\partial^2 u_1}{\partial x'^2_2} + \frac{\partial^2 u_1}{\partial x'^3_3} \tag{41}$$

$$\frac{\partial u_2}{\partial t} - t\frac{\partial p}{\partial x'_1} + \frac{\partial p}{\partial x'_2} = \left(1+t^2\right)\frac{\partial^2 u_2}{\partial x'^2_1} - 2t\frac{\partial^2 u_2}{\partial x'_1 \partial x'_2} + \frac{\partial^2 u_2}{\partial x'^2_2} + \frac{\partial^2 u_2}{\partial x'^2_3} \tag{42}$$

$$\frac{\partial u_3}{\partial t} + \frac{\partial p}{\partial x'_3} = \left(1+t^2\right)\frac{\partial^2 u_3}{\partial x'^2_1} - 2t\frac{\partial^2 u_3}{\partial x'_1 \partial x'_2} + \frac{\partial^2 u_3}{\partial x'^2_2} + \frac{\partial^2 u_3}{\partial x'^2_3} \tag{43}$$

The linear approximation is based on the assumption that the nonlinear terms $u_j \frac{\partial u_i}{\partial x_j}$, in the disturbance momentum equations, can be neglected with respect to both the viscous term $\nu\nabla^2 u_i$ and the mean shear term $u_j \partial U_i/\partial x_j$. This approximation remains valid as long as the amplitude of the disturbance velocity remains small compared with the velocity scale $\sqrt{\nu S}$.

An arbitrary solution of this system in the moving frame can be written as a linear superposition

$$\begin{aligned} u_j(\mathbf{x}', t) &= \int d^3\mathbf{k}\ f_j(\mathbf{k}, t) e^{i\mathbf{k}\cdot\mathbf{x}'} \\ p(\mathbf{x}', t) &= \int d^3\mathbf{k}\ p(\mathbf{k}, t) e^{i\mathbf{k}\cdot\mathbf{x}'}, \end{aligned} \tag{44}$$

where the mode amplitudes $f_j(\mathbf{k}, t)$ and $p(\mathbf{k}, t)$ satisfy

$$k_1 f_1 + k'_2 f_2 + k_3 f_3 = 0 \tag{45}$$

$$\dot{f}_1 + f_2 + ik_1 p = -\mathcal{K}^2 f_1 \tag{46}$$

$$\dot{f}_2 + ik'_2 p = -\mathcal{K}^2 f_2 \tag{47}$$

$$\dot{f}_3 + ik_3 p = -\mathcal{K}^2 f_3 \ , \tag{48}$$

with $k'_2 = k_2 - tk_1$, $\mathcal{K}^2 = k_1^2 + k_2'^2 + k_3^2$, and the wave numbers (k_1, k_2, k_3) are constant in time. The solution for the velocity disturbance modes can be written in the form

$$f_i(\mathbf{k}, t) = M_{ij}(\mathbf{k}, t) f_j(\mathbf{k}, 0) e^{-q(\mathbf{k},t)} \ , \tag{49}$$

where the exponent

$$q(\mathbf{k},t) = \int \mathcal{K}^2 \, dt = \frac{1}{3}k_1^2 \, t^3 \; - \; k_1 k_2 \, t^2 \; + \; (k_i k_i)\, t \tag{50}$$

arises from the viscous damping of all modes. The transfer matrix M has non-vanishing components

$$\begin{aligned} M_{11} &= M_{33} = 1 \\ M_{22} &= \frac{k^2}{\mathcal{K}^2} \\ M_{12} &= \frac{k_3^2 k^2 \, (\Theta - \Theta_0)}{k_1 k_H^3} + \frac{k_1^2 t(k_1^2 - k_2 k_2' + k_3^2)}{k_H^2 \mathcal{K}^2} \\ M_{32} &= \frac{k_3 k^2 (\Theta_0 - \Theta)}{k_H^3} + \frac{k_1 k_3 t(k_1^2 - k_2 k_2' + k_3^2)}{k_H^2 \mathcal{K}^2}, \end{aligned} \tag{51}$$

with

$$k_H = \left(k_1^2 + k_3^2\right)^{\frac{1}{2}}, \quad \Theta_0 = \tan^{-1}\left(\frac{k_2}{k_H}\right), \quad \Theta = \tan^{-1}\left(\frac{k_2'}{k_H}\right) \tag{52}$$

The initial mode amplitudes $f_i(\mathbf{k},0)$ are elements of an ensemble with mean zero and a covariance $\langle f_i(\mathbf{k},0) f_j(\mathbf{l},0)\rangle$. Assuming that the initial disturbance field is homogeneous, isotropic, and has finite energy K_0, the initial covariance is given by the same expression as above for the case of zero mean shear with no boundary

$$\langle f_i(\mathbf{k},0) f_j(\mathbf{l},0)\rangle = \delta^3(\mathbf{k}+\mathbf{l})\left(\delta_{ij} - \frac{k_i k_j}{k^2}\right) K_0 \mathcal{P}(\mathbf{k}), \tag{53}$$

where

$$\mathcal{P}(\mathbf{k}) = \frac{2}{3}\left(\frac{a^5}{\pi^3}\right)^{1/2} k^2 e^{-ak^2} \tag{54}$$

is the probability distribution for disturbance second-moments, and the parameter a, related to the variance of the distribution, will be given a physical interpretation in what follows. This probability distribution is consistent with a k^4 low wave number behavior for the energy spectrum $E(k)$ (Batchelor and Proudman, 1956) and, in the case of linear disturbances in zero-mean-shear flow, leads to a $t^{-\frac{5}{2}}$ decay law for the mean disturbance kinetic energy.

The disturbance mode covariance is related to the energy spectrum tensor by

$$\langle f_i(\mathbf{k},t) f_j(\mathbf{l},t)\rangle = E_{ij}(\mathbf{k},t)\delta^3(\mathbf{k}+\mathbf{l}), \tag{55}$$

so it follows from Eq.(49) that

$$E_{ij}(\mathbf{k},t) = M_{il}(\mathbf{k},t) M_{jm}(\mathbf{k},t) E_{0lm}(\mathbf{k}) e^{-2q(\mathbf{k},t)}, \tag{56}$$

where, as a result of (53),

$$E_{0ij}(\mathbf{k}) = E_{ij}(\mathbf{k},0) = \left(\delta_{ij} - \frac{k_i k_j}{k^2}\right) K_0 \mathcal{P}(\mathbf{k}) \tag{57}$$

is the initial energy spectrum tensor.

The energy spectrum tensor is the fundamental quantity from which all disturbance second-moments are derived by integration over wave number space. Of particular interest are the disturbance stress tensor

$$\tau_{ij}(t) = \int d^3\mathbf{k}\ E_{ij}(\mathbf{k},t)\ , \tag{58}$$

the disturbance kinetic energy $K(t) = \tau_{ii}/2$, and the disturbance dissipation rate

$$\varepsilon(t) = \int d^3\mathbf{k}\ \mathcal{K}^2\ E_{ii}(\mathbf{k},t). \tag{59}$$

A physical interpretation can be given to the parameter a, which appears in the probability distribution (54), by performing the integral in (59) at time zero to obtain $\varepsilon_0 = 5K_0/a$. In terms of the dimensional disturbance kinetic energy $\tilde{K} = \nu S K$, and the dimensional dissipation rate $\tilde{\varepsilon} = \nu S^2 \varepsilon$ the parameter a is given by

$$a = 5\left(\frac{S\tilde{K}_0}{\tilde{\varepsilon}_0}\right) = 5\eta_0 \tag{60}$$

It will be shown that this quantity, a ratio of the disturbance time scale to the mean flow time scale, regulates the subsequent growth or decay of linear disturbances in homogeneous shear flow. In the turbulence case, the variable $\eta = S\tilde{K}/\tilde{\varepsilon}$ also plays a critical role. Jongen and Gatski (1998) have shown that for turbulent homogeneous shear flow, η reaches an equilibrium value which can be analytically connected to the variation of the ratio of kinetic energy production to dissipation rate.

5 Modeled Disturbance Transport Equations

The ensemble-mean kinetic energy and dissipation rate for linear disturbances satisfy evolution equations which can be derived from the linearized Navier-Stokes equations (in the fixed frame). In this homogeneous flow, gradients of all ensemble-mean quantities vanish, and the (dimensionless) kinetic energy and dissipation rate equations reduce to

$$\dot{K} = -\tau_{12} - \varepsilon = \mathcal{P}_K - \varepsilon, \tag{61}$$

$$\dot{\varepsilon} = \mathcal{P}_\varepsilon - \mathcal{D}_\varepsilon, \tag{62}$$

where $\mathcal{P}_K(= -\tau_{12})$ is the kinetic energy production,

$$\begin{aligned}\mathcal{P}_\varepsilon &= -2\left(\left\langle \frac{\partial u_i}{\partial x_1}\frac{\partial u_i}{\partial x_2}\right\rangle + \left\langle \frac{\partial u_1}{\partial x_i}\frac{\partial u_2}{\partial x_i}\right\rangle\right) \\ &= -2\int d^3\mathbf{k}\left[k_1 k_2'\ E_{ii} + \mathcal{K}^2\ E_{12}\right]\end{aligned} \tag{63}$$

is the production-of-dissipation, and

$$\mathcal{D}_\varepsilon = 2\left\langle \frac{\partial^2 u_i}{\partial x_j \partial x_k}\frac{\partial^2 u_i}{\partial x_j \partial x_k}\right\rangle = 2\int d^3\mathbf{k}\mathcal{K}^4\ E_{ii} \tag{64}$$

is the destruction-of-dissipation. From Eqs. (61) and (62), it is seen that only the disturbance dissipation rate equation requires closure models. In the standard $K-\varepsilon$ formulation, the production-of-dissipation is modeled by

$$\mathcal{P}_\varepsilon = -C_{\varepsilon 1}\frac{\varepsilon}{K}\tau_{12}, \tag{65}$$

which gives

$$C_{\varepsilon 1} = -\mathcal{P}_\varepsilon\frac{K}{\varepsilon\tau_{12}} = \frac{K}{\varepsilon}\frac{\mathcal{P}_\varepsilon}{\mathcal{P}_K}, \tag{66}$$

for the production-of-dissipation coefficient. The destruction-of-dissipation is modeled by

$$\mathcal{D}_\varepsilon = C_{\varepsilon 2}\frac{\varepsilon^2}{K}, \tag{67}$$

which yields

$$C_{\varepsilon 2} = \frac{K}{\varepsilon^2}\mathcal{D}_\varepsilon \tag{68}$$

for the destruction-of-dissipation coefficient.

Recall that the components E_{ij} of the energy spectrum tensor are completely defined by Eqs. (49) through (57). With the solution of these equations, all the quantities of interest, including $\mathcal{P}_\varepsilon$ and $\mathcal{D}_\varepsilon$, can be obtained by carrying out the integration in Eqs. (58), (59), (63), and (64). These three-dimensional integrations were initially performed numerically using cubic and spherical grids. It was found that although the convergence was good at small times, at times greater than about $10S^{-1}$, the results became strongly dependent on the grid resolution used (even for grids with as many as 250 million points). The numerical evaluation of the integrals in Eqs. (58), (59), (63), and (64) is therefore greatly simplified, and the accuracy significantly enhanced, by performing the radial integration analytically.

It is convenient to introduce spherical coordinates (k,θ,ϕ), in wave-vector space, such that

$$k_1 = k\sin\theta\cos\phi, \quad k_2 = k\cos\theta, \quad k_3 = k\sin\theta\sin\phi,$$

and $k_H = k\sin\theta$. For the chosen probability distribution (54) the radial integrals in Eqs. (58), (59), (63), and (64) are Gaussian and can easily be carried out analytically. The ensemble-averaged disturbance stress components are then given by

$$\tau_{ij}(t) = \frac{K_0}{4\pi}\int_0^\pi d\theta\sin\theta\int_0^{2\pi} d\phi f^{-\frac{5}{2}}e_{ij}, \tag{69}$$

where the angular functions $f = f(\theta,\phi,t)$, and $e_{ij} = e_{ij}(\theta,\phi,t)$ are defined in the Appendix in Eq. (A1) and Eqs. (A2) to (A6), respectively. This yields for the ensemble-averaged kinetic energy

$$K(t) = \frac{K_0}{8\pi}\int_0^\pi d\theta\sin\theta\int_0^{2\pi} d\phi f^{-\frac{5}{2}}e_{ii}, \tag{70}$$

and for the ensemble-averaged disturbance dissipation rate

$$\varepsilon(t) = \frac{K_0}{8\pi\eta_0}\int_0^\pi d\theta\sin\theta\int_0^{2\pi} d\phi f^{-\frac{7}{2}}e_{ii}p \tag{71}$$

where $p = \mathcal{K}^2/k^2$ so that

$$p = p(\theta, \phi, t) = 1 - t \sin 2\theta \cos\phi + t^2 \sin^2\theta \cos^2\phi \tag{72}$$

The resulting expressions for the production-of-dissipation $\mathcal{P}_\varepsilon$, and destruction-of-dissipation $\mathcal{D}_\varepsilon$ are

$$\mathcal{P}_\varepsilon(t) = -\frac{K_0}{4\pi\eta_0} \int_0^\pi d\theta \sin\theta \int_0^{2\pi} d\phi f^{-\frac{7}{2}} [e_{ii} s + e_{12} p], \tag{73}$$

$$\mathcal{D}_\varepsilon(t) = \frac{7K_0}{40\pi\eta_0^2} \int_0^\pi d\theta \sin\theta \int_0^{2\pi} d\phi f^{-\frac{9}{2}} e_{ii} p^2, \tag{74}$$

respectively, where

$$s = s(\theta, \phi, t) = \frac{1}{2} \sin 2\theta \cos\phi - t \sin^2\theta \cos^2\phi \tag{75}$$

Convergence tests show that these integrals had to be evaluated on grids with spacing of $1/16$ of a degree. With the evaluation of the integrals in Eqs. (69) - (71), Eqs. (73) and (74), it is now possible to analyze the ensemble-averaged transport equations for the disturbance kinetic energy and dissipation rate. Of particular interest is the dissipation rate equation Eq. (62) which requires closure. It will be shown in the next section that closure models for $\mathcal{P}_\varepsilon$ and $\mathcal{D}_\varepsilon$, can be determined through an analysis of the long-time behavior of the disturbance correlations.

6 Results

From an examination of Eqs. (69) - (74), it is apparent that the only factor containing the parameter η_0 is $f(\theta, \phi, t)$, given in Eq. (A1). This factor, which appears in all the ensemble-averaged correlations and which arises from viscous effects, governs the large-time behavior of all correlations causing them to ultimately decay. At large times and generic angles $\sin\theta\cos\phi \approx \mathcal{O}(1)$, the t^3-term in f dominates, leading to negligibly small values of the integrand. However, for $\sin\theta\cos\phi = k_1/k$ small, f is proportional to t at large times. The t^2- and t^3-terms in f will also be $\mathcal{O}(t)$ when (θ, ϕ) lies in a band of solid angle of width $\mathcal{O}(t^{-1})$ about the $k_1 = 0$ plane. At large times, this band of solid angle gives the dominant contribution to the integrals in Eqs. (69) - (74).

Now, consider the disturbance kinetic energy (70). While $f^{-5/2}$ decays at all times, the factor e_{ii} (see Eq. (A5)) grows, indicating that the evolution of the disturbance energy is governed by a relative balance of the two factors. Figure 1 shows the evolution of the disturbance kinetic energy for different initial values of η_0. For a small value of η_0 ($= 0.6$), the factor $f^{-5/2}$ dominates and the energy decays monotonically in time. A transition between this monotonic decay and substantial growth of the disturbance energy occurs for values of η_0 between 1.2, where the energy reaches a minimum and grows briefly, and 2.4, where the energy grows to a magnitude just equal to its initial value before decreasing. For larger values of η_0 (> 3.0), the viscous decay factor is further suppressed and, after a brief initial period of decay, the energy then grows for a period of time before finally decaying. These larger values of η_0 can be compared to results from the turbulent case. The initial value of $\eta_0 = 6$ is a moderate shear case which corresponds to

the equilibrium value for η in turbulent homogeneous shear flow. The temporal evolution shown in Fig. 1 for this value of η_0 contrasts with the exponential energetic growth (Tavoularis, 1985) characteristic of the turbulent case. Here the disturbance kinetic energy grows to a little beyond three times its initial value. Therefore, if the initial disturbance kinetic energy is considerably less than the natural energy scale νS, the linear approximation should remain valid for all times. Calculations have also been carried out for $\eta_0 = 12$ and 18. The evolution of K with time for these other η_0 values (not shown) is very similar to that for $\eta_0 = 6$. The only difference is that, as expected, the maximum value of K reached before the final decay is larger than for $\eta_0 = 6$; for $\eta_0 = 12$, $K_{max} = 6.95K_0$, and for $\eta_0 = 18$, $K_{max} = 10.82K_0$. The initial value of $\eta_0 = 18$ is a high-shear case which is very close to the value used in the DNS study of Lee et al. (1990) ($\eta_0 \approx 17$). Using the numerical simulation results, Lee et al. also compared with RDT and found very good agreement over the time interval examined ($0 \leq t \leq 12$). (The quantitative basis of comparison between the DNS and RDT were the Reynolds stress anisotropy components which are discussed below and shown in Fig. 4. The high-shear limiting value $\eta_0 \to \infty$ corresponds to the case traditionally considered in RDT calculations (Hunt and Carruthers, 1990; Rogers, 1991), where viscosity is neglected. The absence of viscosity allows the energy to grow monotonically, rendering at some finite time the linear approximation invalid.

Figure 2 shows qualitatively similar trends for the disturbance dissipation rate $\varepsilon(t)$ at the corresponding values of $\eta_0 = 0.6$ and 6.0. For the small initial value $\eta_0 = 0.6$, the dissipation rate also decays monotonically. At the moderate shear rate value $\eta_0 = 6$, $\varepsilon(t)$ grows after a brief initial period of decay, reaches a peak and then decays at a more rapid rate than the disturbance kinetic energy. The more rapid decay of $\varepsilon(t)$ compared with $K(t)$, at large times, comes about because $f^{-\frac{7}{2}}$ appears in the integral (71) for the dissipation rate, while the lower power $f^{-\frac{5}{2}}$ appears in (70) for the kinetic energy. Similar behavior was found for the higher shear cases of $\eta_0 = 12$ and 18.

Equation (61) describes the evolution of the disturbance kinetic energy with time. The equation shows that for $\mathcal{P}_K/\varepsilon$ ratios less than one, the kinetic energy must be a decaying function of time. Figure 3 shows that for the very weak shear initial condition of $\eta_0 = 0.6$, the $\mathcal{P}_K/\varepsilon$ ratio never reaches unity confirming the continuous energetic decay of the disturbances. However, for the initial condition $\eta_0 = 6$, 12 and 18, the $\mathcal{P}_K/\varepsilon$ ratio exceeds unity for a period of time and then decays below unity. This latter behavior is reflected in the disturbance energy evolution shown in Fig. 1 for $\eta_0 = 6$ where the disturbance energy grows up to a time of approximately 25 ($\mathcal{P}_K/\varepsilon > 1$) and then decays ($\mathcal{P}_K/\varepsilon < 1$) at larger times. This same qualitative behavior holds for the higher shear rate cases of η_0 of 12 and 18 as well.

Since the main focus here is on disturbances which can eventually grow (and lead to turbulence), the results for the initial value of $\eta_0 = 0.6$ are not of interest. In addition, while this weak shear case yields decaying disturbances, the validity of neglecting the nonlinear terms does come into question. As Cambon and Scott (1999) have pointed out, the contribution of the nonlinear term, while small, may have a cumulative effect on the dynamics over a period of time. In addition, the linearized, weak shear case may be inconsistent because the product term containing the weak mean shear is retained while the nonlinear terms, possibly of the same

magnitude, are omitted. These considerations dictate that subsequent results will focus on the moderate- and high-shear cases.

Figure 4 shows the evolution of the ensemble-mean stress anisotropies

$$b_{ij}(t) = \frac{\tau_{ij}(t)}{2K(t)} - \frac{\delta_{ij}}{3}, \tag{76}$$

for the initial condition $\eta_0 = 6.0$. It is seen that initially isotropic linear disturbances are distorted by mean shear, rapidly becoming anisotropic. The stress anisotropies asymptote to the values $b_{11} = 0.631$, $b_{22} = -0.333$, $b_{33} = -0.298$, and $b_{12} = -0.008$, which is consistent with the turbulent DNS (and RDT) results (Lee, *et al*, 1990) at high-shear rates. In the current study, the b_{11}, b_{22}, and b_{33} anisotropy components are computed individually. The resulting trace ($b_{ii} = 0$) is then used as a measure of the accuracy of the simulation which, for the results presented here, was satisfied to $\mathcal{O}(10^{-15})$.

Recall that initially, an isotropic distribution of the disturbance energy is assumed. Thus, the structure of the disturbance field is significantly altered by the imposition of the mean shear. This alteration is easily seen in the mapping of the anisotropy invariants $II(= -b_{ij}b_{ij}/2)$ and $III(= b_{ik}b_{kl}b_{lj}/3)$ shown in Fig. 5. The figure shows that after $t \approx 2$, the (realizable) disturbance field migrates toward the two-component (2C) state. After $t \approx 10$ the disturbance field is 2C and monotonically evolves towards a one-component (1C) state. Also shown in Fig. 5 is the invariant map trajectory of the DNS results (Lee, *et al*, 1990). As can be seen, at early times ($t \lesssim 2$) both the DNS trajectory and that from the present calculations, with $\eta_0 = 6$ and 18, are in phase, and at later times, even though the DNS evolution lags behind the the current results, all of these evolve toward the same 1C state. At large times, the system has evolved to what has been termed a "statistical eigensolution" of the moments (Hunt and Carruthers, 1990). That is, if the disturbances were to have these forms initially, the disturbance field would change little under a distortion. While the results shown in Fig. 5 are for the $\eta_0 = 6$ and 18 cases, the same trend toward a 1C limit was found to hold for the case of $\eta_0 = 0.6$. Thus, for linear disturbances the existence of the statistical eigensolution is not limited to the high-shear case. These disturbance field results are in sharp contrast to the equilibrium state reached for the turbulent case where the fixed point invariant values are $III_\infty \approx 0.0043$ and $II_\infty \approx 0.064$. These values are far removed from the 2C and 1C states exhibited by the linear disturbance field.

The results up to this point have ascribed a structure to the linear disturbance field in homogeneous shear which differs from the turbulent homogeneous shear case. In addition, the time scale ratio η does not evolve (see Fig. 6) to a constant value, as in the turbulent case, but displays linear algebraic growth at large times. For a particular homogeneous flow (Jongen and Gatski, 1998) , the dynamical behavior of the system can be described by the time scale ratio η, and the production-to-dissipation rate ratio $\mathcal{P}_K/\varepsilon$ discussed previously.

The consequences of these results for developing a closure model for the disturbance dissipation rate equation (62) can be seen from the evolution equation for η given by

$$\dot{\eta} = -(C_{\varepsilon 1} - 1)\frac{\mathcal{P}_K}{\varepsilon} + (C_{\varepsilon 2} - 1), \tag{77}$$

As seen from Fig. 6, η displays a linear behavior at large times so that $\dot{\eta}$ (= 0.34, for $\eta_0 = 6$) is constant. The large time value of $\dot{\eta}$ is nonzero and depends weakly on η_0. This is in contrast to the turbulent case where at large times $\dot{\eta} = 0$. Since the production-to-dissipation rate ratio is not constant (see Fig. 3), Eq. (77) suggests that the closure coefficients $C_{\varepsilon 1}$ and $C_{\varepsilon 2}$ may also be functions of time. Figure 7 shows the evolution of the disturbance dissipation rate coefficients. Results for three initial values of η_0 are shown which suggest that a limiting range of values at large times (and large η_0) can be reached. For $C_{\varepsilon 1}$ there is a modest change in the value at $t = 50$ with changes in η_0: for $\eta_0 = 6$, $C_{\varepsilon 1} = 2.23$, for $\eta_0 = 12$, $C_{\varepsilon 1} = 2.08$, and for $\eta_0 = 18$, $C_{\varepsilon 1} = 2.01$. For $C_{\varepsilon 2}$, the values range about $\pm 3\%$ from a mean of 2.46. Although it was not possible to determine analytically the limiting values for $C_{\varepsilon 1}$ and $C_{\varepsilon 2}$, numerical simulations for large values of η_0 at large times showed that the limiting values were $C_{\varepsilon 1} \approx 2.0$ and $C_{\varepsilon 2} \approx 2.5$. These values are in contrast to the usual values obtained for turbulent closure models where $C_{\varepsilon 1} \approx 1.45$ and $C_{\varepsilon 2}$ lies in the range of 1.83 to 1.92.

In the turbulent case, the destruction-of-dissipation coefficient was deduced from an analysis of the decay of isotropic turbulence (e.g. Comte-Bellot and Corrsin, 1971). In the analysis of the decay of homogeneous, isotropic linear disturbances, above, a value for $C_{\varepsilon 2}$ of 1.4 was determined in a boundary-free case. This is in sharp contrast to the value of 2.5 found in this homogeneous shear flow. An explanation for this difference may lie in the structure of the disturbance field. In the previous decay studies, the disturbance field was isotropic, and remained isotropic in the absence of mean shear. However, as the results shown here indicate, the imposition of mean shear quickly produces an anisotropic field (see Fig. 4) which eventually drives the flow close to a 1C state (Fig. 5). Thus, a more relevant flow with which to form a comparison may be the decay of anisotropic turbulence. Dakos and Gibson (1990) studied such a flow and deduced from the decay of the turbulence the destruction-of-dissipation rate coefficient $C_{\varepsilon 2}$. Their anisotropic decay data yielded a value for $C_{\varepsilon 2}$ of 2.18 which is relatively close to the value of 2.5 found here for $C_{\varepsilon 2}$. Of course, in spite of fundamental differences in the dynamics associated with each study, it is interesting to note that the introduction of anisotropy in either disturbance field (linear or turbulent) significantly increases the value of the coefficient $C_{\varepsilon 2}$.

The value of the production-of-dissipation rate coefficient $C_{\varepsilon 1}$ used in turbulence modeling is determined from a consistency criterion found from homogeneous shear flow at equilibrium. As alluded to earlier, the time scale ratio η is constant ($\dot{\eta} = 0$) in the turbulence case so that Eq. (77) yields the well-known relation

$$\left(\frac{\mathcal{P}_K}{\varepsilon}\right)_\infty = \frac{C_{\varepsilon 2} - 1}{C_{\varepsilon 1} - 1}. \tag{78}$$

With the value of $\mathcal{P}_K/\varepsilon$ fixed from experiments (for example), and $C_{\varepsilon 2}$ fixed from the decay of isotropic turbulence, the value of $C_{\varepsilon 1}$ can be determined. Unfortunately, this is not the case here and, as Fig. 7 shows, the value of $C_{\varepsilon 1}$ varies with time. As noted previously, it was not possible to analytically determine the limiting values for $C_{\varepsilon 1}$; however, simulations were run at large values of η_0 and for long times to try to determine its asymptotic limit. These simulations showed that $C_{\varepsilon 1}$ approached 2.0 at long times which is in contrast to the value of $C_{\varepsilon 1} \approx 1.45$ for

the turbulent case. Thus, for both the production-of and destruction-of-dissipation rate models the closure coefficients are significantly larger than the corresponding turbulent values.

7 Summary and Conclusions

This study has introduced an approach to transition modeling in which deterministic solutions of the linearized Navier-Stokes equation are combined with a probability distribution that accounts for the uncertainty in initial conditions to obtain mean transport equations for disturbances in the laminar regime. This approach was applied to the study of decaying disturbances in zero mean-shear flows. The analysis has shown that the linear disturbance field in laminar flow decays at rates which differ from that of the turbulence field. In the boundary-free case, the disturbance kinetic energy decays at a much faster rate of 5/2 than the corresponding turbulent kinetic energy decay rate of ≈ 1.25. This yields a destruction-of-dissipation rate coefficient $C_{\varepsilon 2}$ in the mean dissipation rate transport equation of 1.4 for the linear disturbances and ≈ 1.8 for the turbulence. In the case with a wall boundary, the disturbance kinetic energy decayed at a rate of 2, which is faster than the corresponding turbulent kinetic energy rate of 1.0. This yields a destruction-of-dissipation rate coefficient $C_{\varepsilon 2}$ of 1.5 for the linear disturbances and ≈ 2 for the turbulence. These results are summarized in Table 1 which clearly shows that the wall has the effect of reducing the decay rate of the disturbance energy in both the laminar and turbulent regimes.

Closure models for the production-of-dissipation rate and destruction-of-dissipation rate in a linearized disturbance transport equation for the dissipation rate have been developed. In this study of mean homogeneous shear flow deterministic solutions of the linearized Navier-Stokes equation are combined with a probability distribution that accounts for the uncertainty in initial conditions, to obtain mean transport equations for disturbance correlations in the laminar regime.

The temporal evolution of the disturbance kinetic energy and the disturbance dissipation rate were shown to depend on the magnitude of the initial value of the time scale ratio η. The temporal evolution for both the kinetic energy and dissipation rate was monotonically decaying for values of $\eta_0 < 1.2$. For larger values of η_0, both quantities initially decayed, then grew with time, and then subsequently decayed at large times. This is in contrast to the turbulent, homogeneous shear case where the quantities displayed exponential growth.

Even though the temporal behavior of the disturbance kinetic energy differed from the turbulence case, the disturbance stress anisotropies did reach a steady-state which corresponded to a "statistical eigensolution" of the problem. An analysis of the anisotropy invariant map shows that this eigensolution corresponded to the 1C limit for the disturbance field, which is in contrast to the structure shown by turbulence at equilibrium ($\dot{b}_{ij} = 0$).

In the turbulent, homogeneous shear case, the time scale ratio η is a fixed point of the system; whereas, in the linear disturbance case it was found to have an $\mathcal{O}(t)$ algebraic growth. As in the turbulent case, the evolution equation for $\dot{\eta}$ yields a relation between the $\mathcal{P}_K/\varepsilon$ ratio and the closure coefficients in the disturbance dissipation rate equation. Unlike the turbulence

case, however, the η and $\mathcal{P}_K/\varepsilon$ variables are time dependent which leads to time dependent behavior for dissipation rate coefficients $C_{\varepsilon 1}$ and $C_{\varepsilon 2}$. Nevertheless, limiting values (for large η_0 and at long times) were obtained which yielded values for $C_{\varepsilon 1}$ and $C_{\varepsilon 2}$ that were larger than the corresponding turbulent values.

Appendix

The angular functions $f(\theta,\phi,t)$, and $e_{ij} = e_{ij}(\theta,\phi,t)$ appear in Eqs. (69) to (74), and are given by

$$\begin{aligned} f(\theta,\phi,t) &= 1 + \frac{2}{5\eta_0}\frac{q(\mathbf{k},t)}{k^2} \\ &= 1 + \frac{2}{5\eta_0}\left(t - \frac{1}{2}t^2\sin 2\theta\cos\phi + \frac{1}{3}t^3\sin^2\theta\cos^2\phi\right), \end{aligned} \tag{A1}$$

and

$$\begin{aligned} e_{11}(\theta,\phi,t) &= \left(\cos^2\theta + \sin^2\theta\sin^2\phi\right) \\ &\quad + \left(2\cot\theta\sin^2\phi\right)\alpha + \left(\csc^2\theta\sin^2\phi\tan^2\phi\right)\alpha^2 \\ &\quad - \left(\sin 2\theta\cos^3\phi + 2\alpha\sin^2\phi\cos\phi\right)\frac{rt}{p} \\ &\quad + \sin^2\theta\cos^4\phi\left(\frac{rt}{p}\right)^2, \end{aligned} \tag{A2}$$

$$e_{22}(\theta,\phi,t) = \frac{\sin^2\theta}{p^2}, \tag{A3}$$

$$\begin{aligned} e_{33}(\theta,\phi,t) &= \left(\cos^2\theta + \sin^2\theta\cos^2\phi\right) \\ &\quad - \left(2\cot\theta\sin^2\phi\right)\alpha + \left(\csc^2\theta\sin^2\phi\right)\alpha^2 \\ &\quad - \sin^2\phi\cos\phi\left(\sin 2\theta - 2\alpha\right)\frac{rt}{p} \\ &\quad + \sin^2\theta\cos^2\phi\sin^2\phi\left(\frac{rt}{p}\right)^2, \end{aligned} \tag{A4}$$

$$\begin{aligned} e_{ii}(\theta,\phi,t) &= \left(1 + \cos^2\theta + \frac{\sin^2\theta}{p^2}\right) + \left(\csc^2\theta\tan^2\phi\right)\alpha^2 \\ &\quad - \left(\sin 2\theta\cos\phi\right)\frac{rt}{p} + \sin^2\theta\cos^2\phi\left(\frac{rt}{p}\right)^2, \end{aligned} \tag{A5}$$

$$\begin{aligned} e_{12}(\theta,\phi,t) &= -\frac{\left(\sin 2\theta\cos\phi + 2\alpha\sin\phi\tan\phi\right)}{2p} \\ &\quad + \left(\frac{\sin^2\theta\cos^2\phi}{p}\right)\frac{rt}{p}, \end{aligned} \tag{A6}$$

where $p = p(\theta,\phi,t)$ is given in Eq. (72), and

$$\alpha(\theta,\phi,t) = \tan^{-1}\left(\cot\theta\right) - \tan^{-1}\left(\cot\theta - t\cos\phi\right) \tag{A7}$$

$$r(\theta,\phi,t) = -\cos 2\theta + \frac{t}{2}\sin 2\theta\cos\phi. \tag{A8}$$

Case	p	$C_{\varepsilon 2}$
Laminar-No Wall	2.5	1.4
Laminar-Wall	2.0	1.5
Turbulent-No Wall	≈ 1.10	≈ 1.9
Turbulent-Wall	≈ 1.0	≈ 2.0

Table 1. Decay exponent p and model coefficients $C_{\varepsilon 2}$ for laminar and turbulent cases.

References

Batchelor, G. K. and Townsend A. A., 1948, "Decay of isotropic turbulence in the initial period," *Proc. Roy. Soc. A*, **193**, 539.

Batchelor, G. K. and Proudman I., 1956, "The large-scale structure of homogeneous turbulence," *Phil. Trans. Roy. Soc. London*, **248A**, 369.

Cambon, C. and Scott, J. F., 1999, "Linear and nonlinear models of anisotropic turbulence," *Annu. Rev. Fluid Mech.*, **31**, 1.

Comte-Bellot, G. and Corrsin S., 1966, "The use of a contraction to improve the isotrophy of grid-generated turbulence," *J. Fluid Mech.* **25**, 657.

Comte-Bellot, G. and Corrsin S., 1971, "Simple Eulerian time correlation of full- and narrow-band velocity signals in grid-generated, 'isotropic' turbulence," *J. Fluid Mech.* **48**, 273.

Dakos, T. and Gibson, M. M., 1990, "The decay of anisotropic homogeneous turbulence," In *Engineering Turbulence: Modelling and Experiments*, (W. Rodi and E. N. Ganic eds.), Elsevier, Amsterdam, 73.

Frisch, U., *Turbulence*, 1995, Cambridge University Press, Cambridge.

Grosch, C. E. and Salwen, H., 1978, "The continuous spectrum of the Orr-Sommerfeld equation. Part 1. The spectrum and the eigenfunctions," *J. Fluid Mech.* **87**, 33.

Hinze J., *Turbulence*, 1975, McGraw-Hill, New York.

Hunt, J. C. R. and Graham J. M. R., 1978, "Free-stream turbulence near plane boundaries," *J. Fluid Mech.* **84**, 209.

Hunt, J. C. R. and Carruthers, D. J., 1990, "Rapid distortion theory and the 'Problem' of turbulence," *J. Fluid Mech.*, **212**, 497.

Jongen, T. and Gatski, T. B., 1998, "A new approach to characterizing the equilibrium states of the Reynolds stress anisotropy in homogeneous turbulence," *Theoret. Comput. Fluid Dynamics*, **11**, 31. Erratum: *Theoret. Comput. Fluid Dynamics*, **12**, 71.

Lee, M. J., Kim, J. and Moin, P., 1990, "Structure of turbulence at high shear rate," *J. Fluid Mech.*, **216**, 561.

Lesieur, M., *Turbulence in Fluids*, 1995, Kluwer Academic Publishers, Dordrecht.

J. L. Lumley, *Stochastic Tools in Turbulence*, 1970, Academic Press, New York.

B. Perot and P. Moin, "Shear-free turbulent boundary layers. Part 1. Physical insights into near-wall turbulence," *J. Fluid Mech.*, **295**, 199.

Rogallo, R. S., 1984, "Numerical Experiments in Homogeneous Turbulence," *NASA Technical Memorandum 81315.*

Rogers, M. M. and Moin, P., 1987, "Structure of the vorticity field in homogeneous turbulent flows," *J. Fluid Mech.*, **176**, 33.

Rogers, M. M., 1991, "The structure of a passive scalar field with a uniform mean gradient in rapidly sheared homogeneous turbulent flow" *Phys. Fluids A*, **3**, 144.

Salhi, A., Cambon, C. and Speziale, C. G., 1997, "Linear Stability Analysis of Plane Quadratic Flows in a Rotating Frame with Applications to Modeling," *Phys. Fluids*, 9, 2300.

Salwen, H. and Grosch, C. E., 1981, "The continuous spectrum of the Orr-Sommerfeld equation. Part 1. Eigenfunction expansions," *J. Fluid Mech.*, **104**, 445.

Speziale, C. G., Abid, R. and Blaisdell, G. A., 1996, "On the consistency of Reynolds stress turbulence closures with hydrodynamic stability theory," *Phys. Fluids*, **8**, 781.

Tavoularis, S. and Corrsin, S., 1981, "Experiments in nearly homogeneous turbulent shear flow with a uniform mean temperature gradient. Part 2. The fine structure," *J. Fluid Mech.*, **104**, 349.

Tavoularis, S., 1985, "Asymptotic laws for transversely homogeneous turbulent shear flows," *Phys. Fluids*, **28**, 999.

Tavoularis, S. and Karnik, U., 1989, "Further experiments on the evolution of turbulent stresses and Scales in uniformly sheared turbulence," *J. Fluid Mech.*, **204**, 457.

Thomas, N. H. and Hancock, P. E., 1977, "Grid turbulence near a moving wall," *J. Fluid Mech.*, **82**, 481.

Townsend, A. A., 1970, "Entrainment and the structure of turbulent flow," *J. Fluid Mech.*, **41**, 13.

Uzkan, T. and Reynolds W. C., 1967, "A shear-free turbulent boundary layer," *J. Fluid Mech.*, **28**, 803.

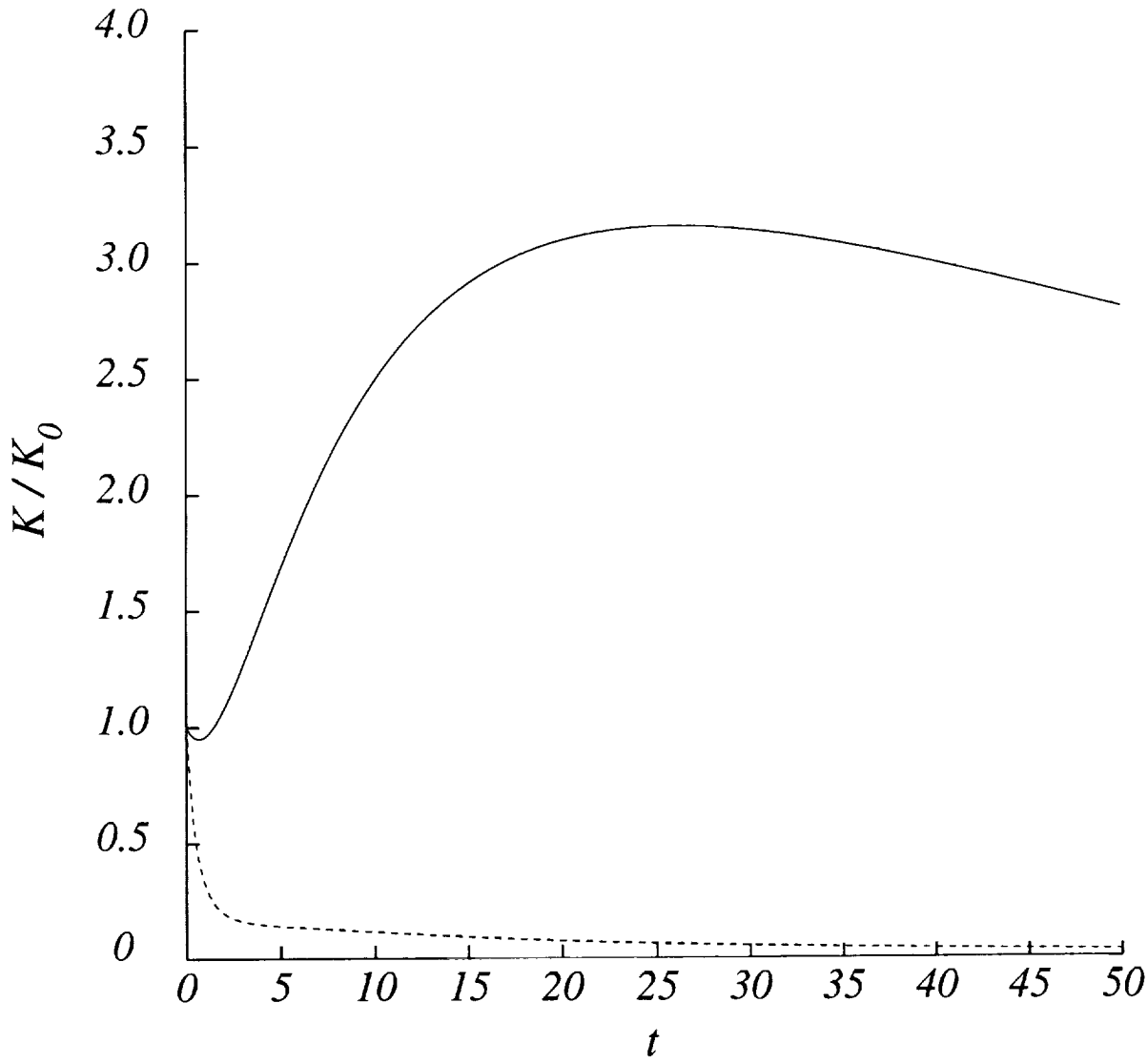

Figure 1: Temporal evolution of disturbance kinetic energy K for initial conditions: $\eta_0 = 0.6$; $\eta_0 = 6$.

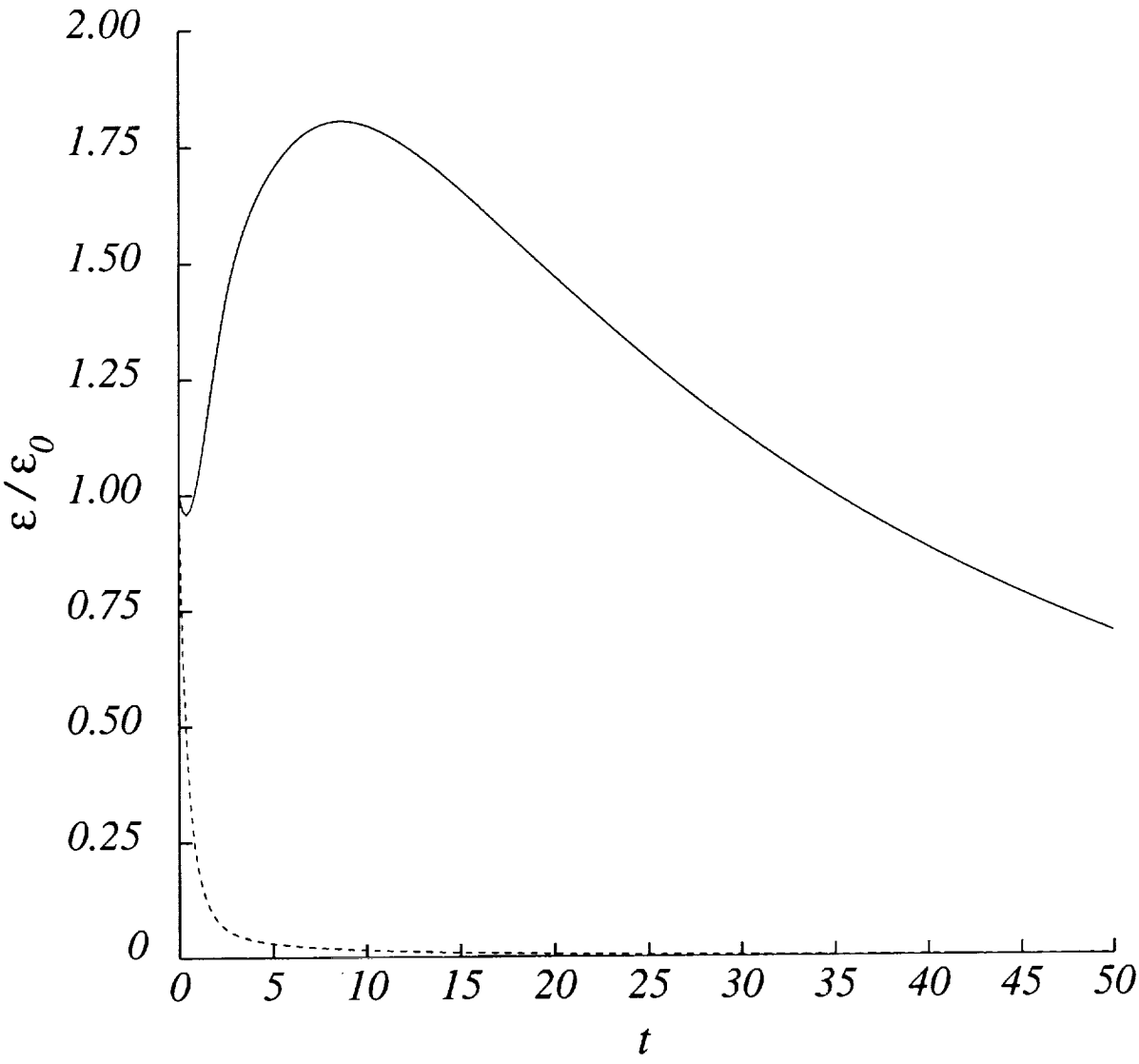

Figure 2: Temporal evolution of disturbance dissipation rate ε for initial conditions: $\eta_0 = 0.6$; $\eta_0 = 6$.

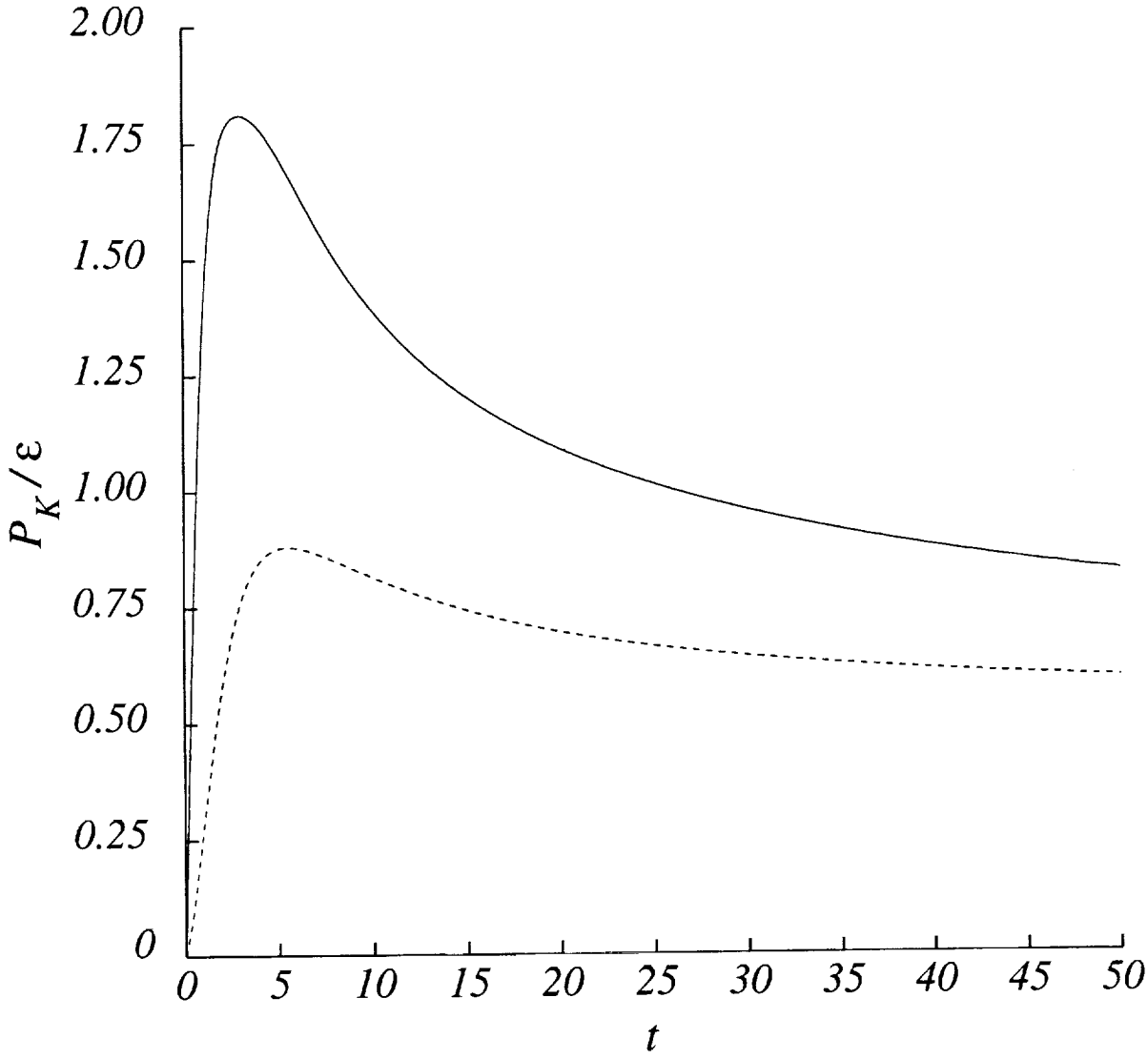

Figure 3: Temporal evolution of production-to-dissipation rate ratio $\mathcal{P}_K/\varepsilon$ for initial conditions: $\eta_0 = 0.6$; $\eta_0 = 6$.

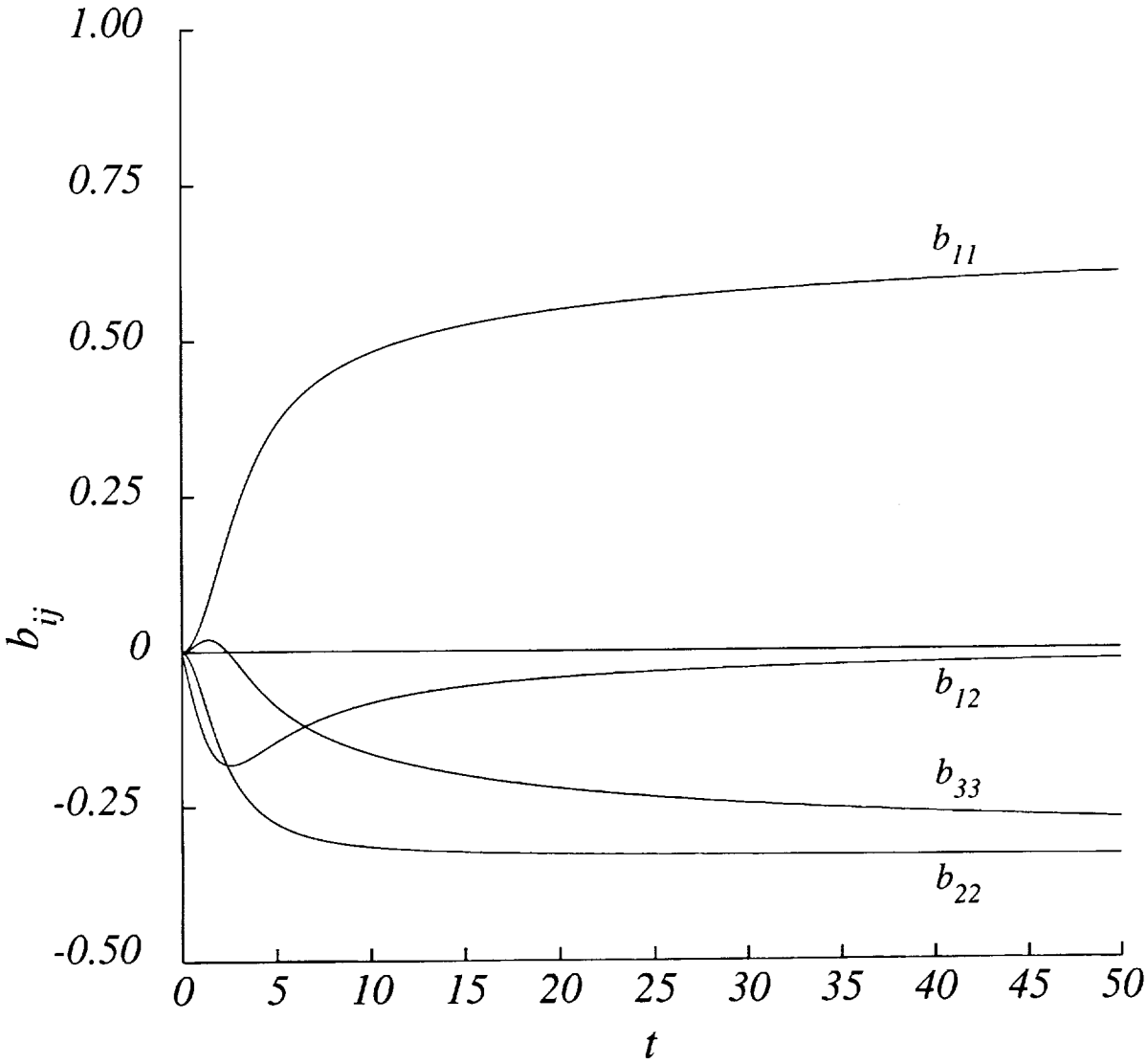

Figure 4: Temporal evolution of disturbance anisotropy tensor b_{ij} for initial condition $\eta_0 = 6$.

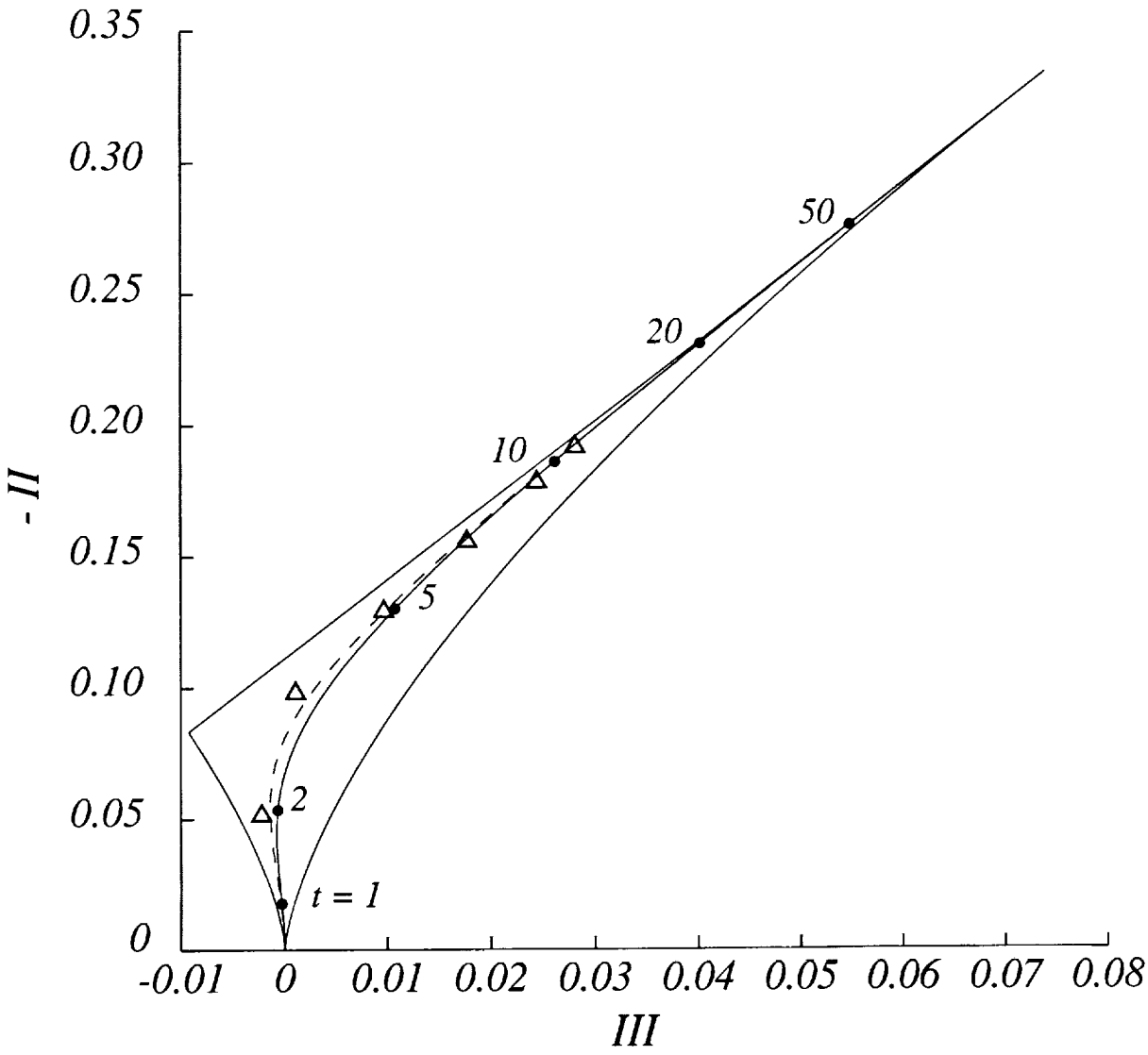

Figure 5: Invariant mapping of disturbance anisotropy tensor at various times for initial conditions: $\eta_0 = 6$ (times as labeled); $\eta_0 = 18$; $\triangle$, $\eta_0 \approx 17$ from DNS (Lee, *et al*, 1990) at $t = 2, 4, 6, 8, 10, 12$.

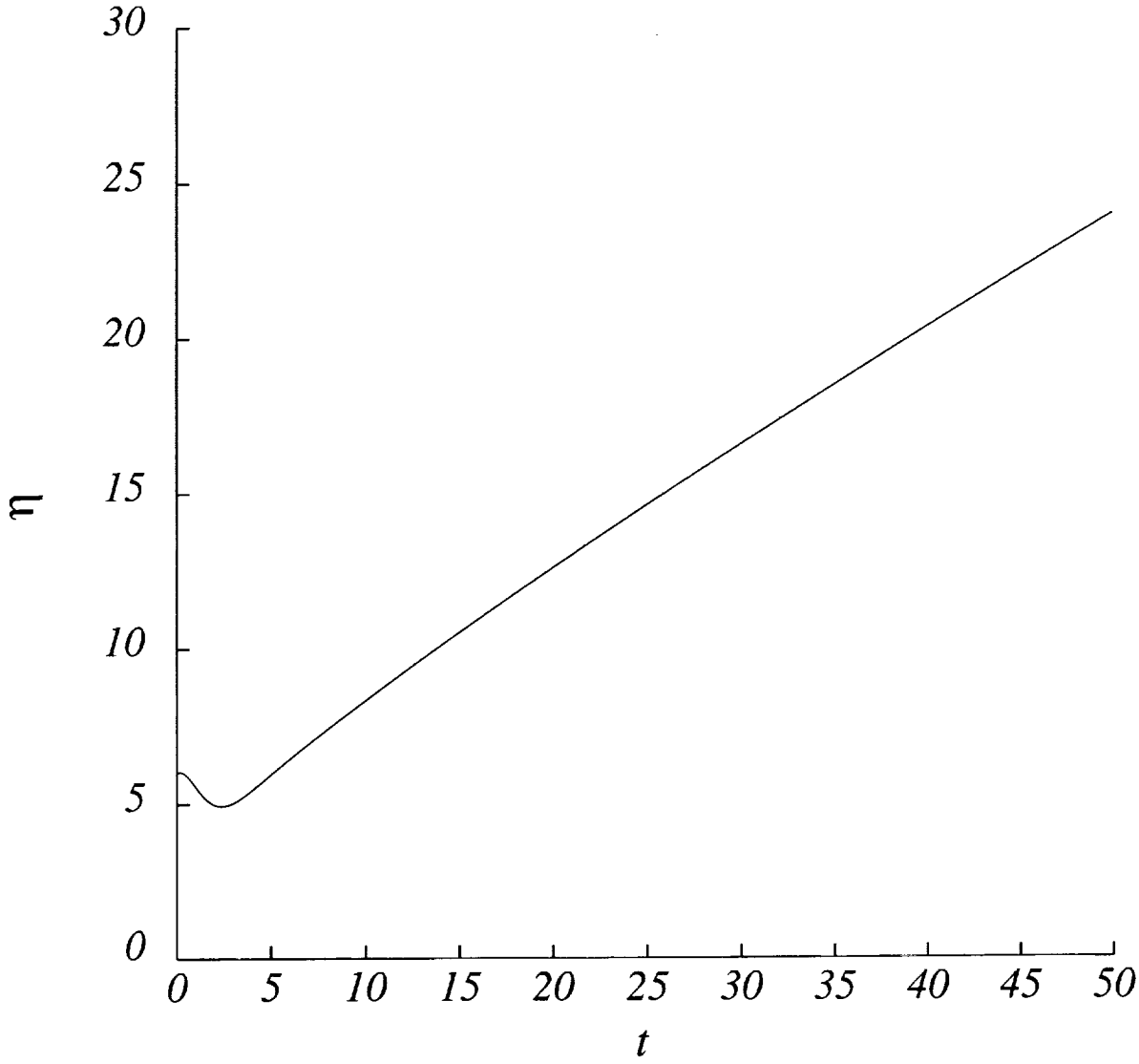

Figure 6: Temporal evolution of time scale ratio η for initial condition $\eta_0 = 6$.

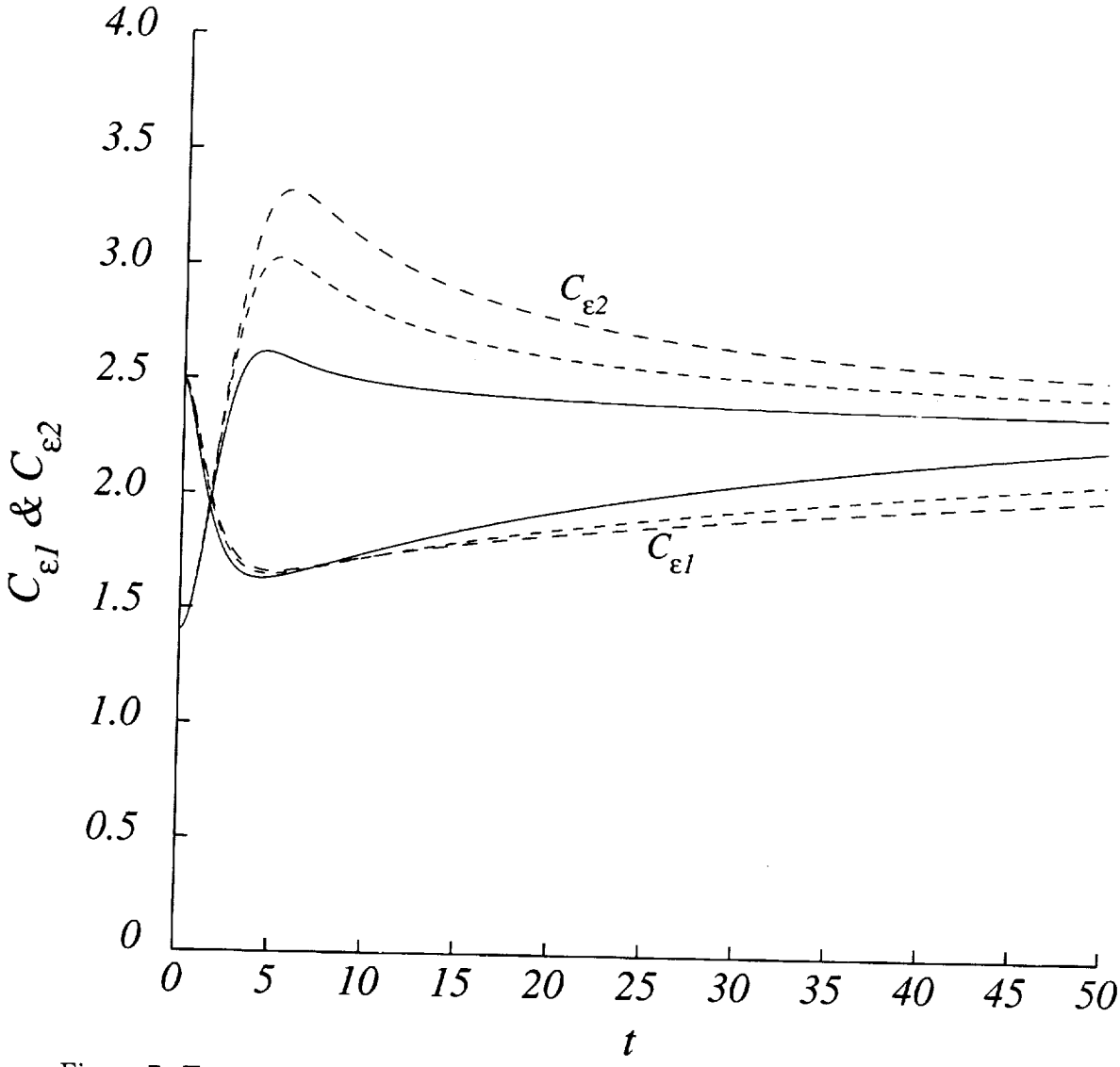

Figure 7: Temporal evolution of closure coefficients $C_{\varepsilon 1}$ and $C_{\varepsilon 2}$ for initial conditions: $\eta_0 = 6$; $\eta_0 = 12$; $\eta_0 = 18$.